Trends in Biomaterials and Artificial Organs
www.biomaterials.org.in/tibao
ISSN 0971-1198
https://doi.org/10.5281/zenodo.16793160

Review Article

A Comprehensive Review of Graphene-Hydroxyapatite Composites: Promising Biomaterials for Bone Tissue Regeneration

Othmane Khalifi Taghzouti

Faculty of Science, Ign Tofail University, Kenitra, Morocco

Received: *22 October 2024*
Accepted: *12 February 2025*
Published online: *31 July 2025*

Keywords: *graphene, hydroxyapatite composite, biomaterial, tissue regeneration*

Graphene family materials (GFMs) integrated with hydroxyapatite (HA) stand as compelling biomaterials for bone tissue regeneration, owing to their exceptional mechanical and biological attributes. This comprehensive review elucidates recent strides in research dedicated to the GFMs-HA composite, underscoring its potential as a pivotal biomaterial in the realm of bone tissue regeneration. The discourse herein navigates through discerning analyses of optimal strategies and procedural methodologies imperative for circumventing the proclivity of GFMs toward aggregation within organic, hydrate solutions, and the HA matrix. Emphasis is placed on the significance of biomimetic mineralization as an unobtrusive approach for crafting GFMs-HA composites under mild conditions, and a nuanced exposition of the biomimetic mineralization mechanism governing HA crystal formation in the presence of GFMs is provided. Furthermore, the review expounds upon the salient impact of GFMs-HA composites on cellular behavior, encapsulating pivotal facets such as cell proliferation, adhesion, and their proclivity for stimulating osteogenic differentiation. In addition, an insightful exploration into the augmentation of fracture toughness in HA, consequent to the incorporation of GFMs, is deliberated upon, thereby underscoring the potential translational significance of these composites in the domain of bone tissue engineering. This review serves as a compendium of recent advancements, providing a scholarly perspective on the evolving landscape of GFMs-HA composite research, thereby contributing to the broader discourse on biomaterials for bone tissue regeneration.

Introduction

The skeletal framework of the human body, constituting the bone skeleton, is susceptible to fractures and injuries resulting from accidents or conditions such as osteoporosis, osteoarthritis, and myelitis, thereby leading to bone loss. In instances where the intrinsic bone remodeling process proves insufficient for the removal and replacement of bone, the introduction of external biomaterials becomes imperative. Natural biomaterials, including allografts, autografts, and xenografts, exemplify such external materials. However, these natural biomaterials bear the risk of transmitting infections and pathogens between bone donors and recipients.

To circumvent the potential transmission of diseases, synthetic biomaterials present a viable solution, such as metals polymers (e.g., polymethylmethacrylate,polyethylene) [1], bioglasses (e.g., 45S5 bioglass comprising SiO_2, Na_2O, CaO, P_2O_5), and ceramics (e.g., tricalcium phosphate, hydroxyapatite) [2]. Hydroxyapatite (HA), in particular, emerges as an attractive biomaterial for bone regeneration owing to its chemical composition resembling natural bone, biocompatibility, bioactivity, and osteoconductivity [3]. However, despite these favorable attributes, the inherent limitations of HA, such as its diminished ability to stimulate the differentiation and proliferation of osteoblastic cells, as well as its brittleness, impose constraints on its biomedical applications.

An intriguing prospect for overcoming these limitations lies in the potential integration of Graphene Family Materials (GFMs) with HA. This prompts critical questions regarding the consequences of adding GFMs to HA: How does the inclusion of GFMs impact the characteristics of the composite material? What transpires when GFMs-HA comes into contact with cells?

* *Coresponding author*
E-mail address: *khalifi.taghzouti.othmane@gmail.com* (**Dr.** *Othmane Khalifi Taghzouti Faculty of Science, Ibn Tofail University, Kenitra, Morocco)*

Can GFMs enhance the fracture toughness of HA? These inquiries form the focal points of investigation in this context, offering avenues for further exploration and understanding in the realm of biomaterials for bone tissue regeneration.

This review endeavors to underscore recent advancements in the research on graphene family materials-hydroxyapatite as a promising candidate for bone regeneration and implantation. The exposition begins with an overview of graphene family materials, followed by a detailed exploration of the composition, functions of bone, bone remodeling processes, and the characteristics of hydroxyapatite. The subsequent sections delve into chemical strategies and process-mixing methodologies aimed at enhancing the dispersion of GFMs in aqueous and organic solutions, as well as within the HA matrix. The review also introduces the novel concept of biomimetic mineralization of HA crystals in the presence of GFMs as an innovative strategy for fabricating GFMs-HA composites.

Furthermore, the narrative encompasses recent studies elucidating the impact of GFMs on enhancing both the biological and mechanical properties of HA. Finally, a succinct conclusion, along with prospective insights, is presented, encapsulating the current state of knowledge and potential directions for future research in this burgeoning field.

Graphene Family Materials

Graphene, a single atomic layer with a two-dimensional (2D) sp^2 hybridized carbon structure, is arranged in a hexagonal lattice [4,5]. Its remarkable properties, including a Young's modulus of approximately 1 TPa, intrinsic strength of 130 GPa, large specific surface area (2630 $m^2 g^{-1}$), and excellent osteoinductivity, make it an exceptionally robust and promising reinforcement material in hydroxyapatite matrices [6-8]. The extraordinary characteristics of graphene extend its applications to various biomedical fields, such as antibacterial paper, cancer targeting, photothermal therapy, drug delivery, biological imaging, and tissue engineering [9-16].

Research interest has been directed towards graphene family materials (GFMs), encompassing graphene oxide (GO), reduced graphene oxide (rGO), graphene nanosheets (GNS), ultrathin graphite, and few-layer graphene. This focus arises from the diverse characteristics exhibited by each graphene material, including surface chemistry, lateral dimension, quality of graphene sheets, composition, and purity [17]. To alleviate nomenclature confusion, a new classification system has been introduced for GFMs, emphasizing three key characteristics: average lateral dimension, atomic carbon/oxygen ratio, and the number of graphene layers [18].

Recently, graphene oxide, reduced graphene oxide, graphene nanosheets, and few-layer graphene have become prevalent choices as reinforcing agents in hydroxyapatite, as evidenced in the literature. A variety of methods have been developed to generate GFMs, encompassing chemical, mechanical, and electrochemical exfoliation of graphite, epitaxial growth on silicon carbide, thermal reduction, and chemical vapor deposition (CVD) [5,19–26].

Among these methods, the chemical oxidation of graphite followed by exfoliation is the most widely employed technique to produce GO. Hummer's method, involving the oxidation of graphite by reacting it with a mixture of oxidant reagents - sulfuric acid (H_2SO_4) and potassium permanganate ($KMnO_4$) - is commonly used for graphite oxidation [27]. Additionally, to produce GO, exfoliation of graphite oxide can be performed in an organic or hydrate solution to isolate single layers. Furthermore, rGO can be synthesized through reduction reagents such as hydrazine (NH_2NH_2), hydroquinone, or sodium borohydride ($NaBH_4$). Alternatively, eco-friendly approaches utilizing solvothermal, hydrothermal, electrochemical, microwave, flash, ultraviolet, and gamma-irradiation methods have been developed to replace hazardous reducing agents [24,28–31].

Several models have been proposed to elucidate the structure of GO, with Lerf Klinowski's model being widely accepted. This model confirms the presence of aromatic entities, epoxide, and hydroxyl groups on the basal plane, and the experimental verification of carboxylic acid on the edge of graphene has been established through infrared spectroscopy [32–34].

Bone

Composition architecture, function of bone

Bone constitutes living tissue characterized by two matrices: the Cellular Matrix (CM) and the Extracellular Matrix (ECM). The CM is comprised of osteoblast cells, responsible for bone formation, and osteoclast cells, responsible for bone resorption [35]. Additionally, other cells, including osteocytes, border cells, and differentiated osteoblasts, play crucial roles in the bone remodeling process. The ECM, constituting 69% mineral phase, 22% organic phase, and 9% water, primarily features phosphate and calcium as the most abundant minerals, while other cationic and anionic minerals such as Na, Mg, and HPO_4 are present in smaller amounts [36].

Remodeling of bone

Bone remodeling is an inherent and continuous physiological process wherein osteoblast cells are responsible for the removal of aged bone, while osteoclast cells facilitate the replacement with new bone. This remodeling mechanism is crucial for maintaining the mechanical integrity of bone and promoting the regeneration of new bone tissue, particularly in response to fractures [37]. The sequential stages of the bone remodeling cycle unfold as follows: initiation begins with the activation phase occurring on previously inactive surfaces, which become activated in the presence of border cells. Subsequently, the border cells retract, allowing osteoclast cells to fuse and undergo differentiation into active osteoclasts. These osteoclasts then adhere to the bone matrix, initiating the resorption of bone tissue. The enzymatic action degrades the organic component, and the mineral component dissolves via the action of hydrogen ions (H^+). Following the completion of resorption, osteoclast cells undergo apoptosis, leaving behind resorption gaps. In the subsequent phases, osteoblast cells assume the role of gap fillers by generating a new organic matrix comprised of collagen fibers, referred to as a "steroid." This issucceeded by the biomineralization of the mineral matrix. As the process concludes, osteoblasts gradually become less active and undergo differentiation into border cells and osteocytes, contributing to the cyclical nature of bone remodeling.

Hydroxyapatite

Hydroxyapatite (HA), with the chemical formula $Ca_{10}(PO_4)_6(OH)_2$, is a naturally occurring mineral that constitutes the inorganic component of bone tissue in vertebrates. Its resemblance to the mineral phase of bone, combined with its biocompatibility and bioactivity, has led to extensive research into its use in biomedical applications. The unique chemical composition and crystalline structure of HA contribute to its exceptional mechanical strength, thermal stability, and biological performance, making it a promising material for use in orthopedic, dental, and tissue engineering

applications. Additionally, the surface properties of HA can be tailored through various fabrication techniques to enhance its bioactivity and promote osseointegration in medical implants.

Hydroxyapatite (HA) stands as a compelling biomaterial in the domain of hard tissue engineering, utilized for the restoration of damaged bone and the regeneration of bone tissue due to its inherent biological properties and chemical composition, closely resembling that of natural bone [38]. HA is a member of the crystallographic apatite family, and its crystalline structure conforms to the hexagonal system with space group P63/m. The crystallographic parameters defining its structure are as follows: a = 9.424 Å, c = 6.879 Å, â = 120°C and V = 529.09 Å³ [39–41].

The crystallographic arrangement of HA comprises two horizontal layers of PO_4 tetrahedra, situated at the z = 1/4 and z = 3/4 planes. The Ca^{2+} atoms within the structure can be categorized into two types: Ca (I) and Ca (II). Specifically, four calcium atoms designated as Ca (I) are positioned at the z = 0, 1/2 plane, while the six Ca (II) atoms are located at the 1/4, 3/4 planes, with three atoms on each plane. Additionally, two OH ions are situated at the 1/4, 3/4 planes [42].

Chemical strategy and process mixing method to enhance GFMs dispersion in aqueous, organic solution and in HA

The primary challenge lies in achieving the homogeneous dispersion of Graphene Family Materials (GFMs) in both aqueous and organic solutions to prevent the aggregation of GFMs when they are introduced into hydroxyapatite solutions. The ð-ð stacking between layers of graphene induces insolubility in both organic and aqueous

Table 1: Covalent and non-covalent functionalization of graphene

Functionalization	Molecule Kind	Organic molecule	Reaction Kind	Stable Dispersant Solvent	Reference
Covalent functionalization	Thiocarbonate	xanthate	Free Radical grafted	DMF	[50]
	Polymer	6-armed poly (ethylene glycol)	Amidation	Water, PBS	[53]
		Poly (oxyalkylene) mines	Free radical grafting or epoxide ring-opening reaction	THF	[47]
		Poly (tert-butyl acrylate)	radical polymerization	Toluene	[49]
		Poly (ε-caprolactone)	-	CH_2Cl_2	[49]
	Organosilane	Hexadecyltrimethoxysilane,	silanization	CCl_4	[52]
		N-(trimethoxysilylpropyl) ethylenediamine triacetic acid		water	[46]
		3-amino-propyltriethoxysilane		water, ethanol, DMF,DMSO,APTES	[55]
	Organotin	dibutyldimethoxytin	-	CCl_4	[52]
	Amine	Ethylenediamine, 1,6-hexanediamine	Amidation	DMF	[52]
		amines 1-aminopyrene, 2-aminofluorene, aliphatic amine, 1-octadecylamine		isopropanol	[44]
		Octadecylamine, dodecylamine, hexadecylamine		Toluene, chloroform chlorobenzene	[48]
	Isocyanate	4-isocyanatobenzenesulfonyl azide Phenylisocyanate ,4-acytylphenylisocyanate, tert-butyl isocyanate	Carbamation(à verifier)	DMF,NMP,DMSO	[48]
	Nitrile	malononitrile anion	epoxide ring-opening reaction	either organic solvent , water	[45]
Non-Covalent functionalization	Pyrene	Pyrene laterally-grafted oligoether dendron	π-π interactions	water	[61]
		Pyrene-adamantane (1), pyrene-adamantane -methylated β-cyclodextrin (2).		DMF,DMSO,NMP,THF(1), Water (2)	[65]
	Carboxylic acid	9-anthracene carboxylic acid		Water, water-ethanol	[57]
		Pyrene butynic acid		Ethanol, Acetone, DMF, THF, Ethanol, Pyridine, Methanol, Water	[170]
	Co-polymere	poly(3,4-ethylene dioxythiophene):poly(styrene sulfonate)		water	[60]
	DNA	Flavin Mononucleotide			[56]
	Cationic molecule	poly(1-glycidyl-3-methylimidazolium chloride)	Cation- π interaction		[171]
	Surfactant	sodium dodecyl sulfate			[59]
		sodium dodecyl sulfate nonylphenylether			
	Polymer	Pluronic block copolymers F127,and P123			[64]
		N-methyl-2pyrrolidone		Methanol, ethanol, isopropanol, DMF NMP.	[22]
		poly(sodium 4-styrene sulfonate)		THF, cyclohexane, toluene, DMF, ethanol	[63]
		Polythiophene-graft-poly(methyl methacrylate)		DMF	[62]
		polyindole		water	[58]

solvents. Moreover, the inadequate presence of functional organic groups on the graphene surface leads to suboptimal dispersion within the hydroxyapatite (HA) matrix, consequently affecting the properties of the final composite. To address this limitation and ensure homogeneous dispersion while averting agglomeration of GFMs, chemical surface functionalization through dispersant agents has emerged as an effective strategy. This approach proves instrumental in enhancing the dispersion of graphene in organic solvents, ultimately achieving a homogeneous dispersion within the hydroxyapatite matrix.

The chemical functionalization strategy can be categorized into two main types: covalent and non-covalent functionalization (table 1).

Covalent functionalization

Covalent functionalization of graphene involves the attachment of chemical groups or molecules to the graphene surface through covalent bonds. This process is essential for tailoring the properties of graphene and expanding its applicability in various fields, including electronics, energy storage, sensors, and biomedicine. The pristine surface of graphene is chemically inert, limiting its interaction with other materials and applications. Covalent functionalization enables the introduction of specific functionalities onto the graphene surface, thereby enhancing its chemical reactivity, stability, and compatibility with other materials.

A diverse array of organic molecules can be employed as dispersant agents for the covalent functionalization of Graphene Family Materials (GFMs) through strategies such as free radical grafting, amidation, silanization, epoxide ring-opening, radical polymerization, and carbamation reactions, thereby establishing covalent bonds between the functional groups on the surface of GFMs and organic molecules, including thiocarbonate, polymers, organosilanes, phenyl compounds, organotin, amines, isocyanates, and nitriles [42–55].

Non-covalent functionalization of graphene involves the adsorption or interaction of molecules, ions, or nanoparticles onto the graphene surface through non-covalent bonds, such as ð-ð stacking, van der Waals forces, hydrogen bonding, or electrostatic interactions. Unlike covalent functionalization, non-covalent functionalization does not involve the formation of chemical bonds between the functionalizing agents and the graphene surface. Instead, it relies on weak interactions between the molecules and the graphene lattice.

A variety of organic molecules, such as pyrene, carboxylic acid, polymers, co-polymers, DNA, and surfactants, have been utilized as dispersant agents in this context. These solvents include phosphate-buffered saline (PBS), Tetrahydrofuran (THF), toluene, dichloromethane (CH_2Cl_2), carbon tetrachloride (CCl_4), ethanol (EtOH), methanol (MeOH), isopropanol, N, N-dimethylformamide (DMF), dimethyl sulfoxide (DMSO), chloroform ($CHCl_3$), chlorobenzene, (3-Aminopropyl) triethoxysilane (APTES), N-Methyl-2-pyrrolidone (NMP), isopropanol, cyclohexane, acetone, and pyridine [22,56-65]. As a result of both covalent and non-covalent functionalization of GFMs, successful dispersion has been achieved in water, as well as in a wide range of organic solvents.

Similarly, hydroxyapatite is typically prepared in both aqueous solutions and organic solvents [66,67]. However, the stability of hydroxyapatite (HA) in these solvents is crucial due to its propensity for immediate precipitation in both aqueous solutions and organic solvents. Moreover, modifying the surface of hydroxyapatite through the use of dispersant agents has been shown to enhance the dispersion of HA in aqueous solutions and organic solvents [67]. Diverse organic molecules have been investigated as grafted dispersant agents for Hydroxyapatite (HA), leading to effective dispersion of HA in various solvents, including aqueous solutions, chloroform, methylene chloride, and basic solutions [44,67–71].

The fabrication of Graphene Family Materials-Hydroxyapatite (GFMs-HA) composites requires the application of dispersant agents to facilitate the dispersion of each component prior to mixing. For instance, cetyl trimethyl ammonium bromide (CTAB) has been utilized as a dispersant agent to separately disperse graphene and nickel-doped HA in deionized water. Subsequent ball milling served as the mixing method, resulting in the favorable dispersion of graphene within the nanocomposite [72].

On the other hand, the surfaces of Graphene Oxide (GO) and Reduced Graphene Oxide (rGO) are negatively charged due to the presence of organic functional group [73,74]. Simultaneously, the surface of hydroxyapatite (HA) comprises various charged crystallographic surfaces, specifically prismatic ac and bc planes known as the C site (enriched in Ca^{2+}), which are positively charged, and the prismatic ab plane known as the P site (abundant in phosphate groups), which is negatively charged [75,76]. Consequently, the electrostatic interaction between the negatively charged epoxide, hydroxyl, and carboxylic acid functional groups on the surfaces of graphene oxide and reduced graphene oxide allows for easy binding to HA. This interaction occurs with the positively charged calcium sites (C) on the crystallographic surfaces of HA, contributing to a robust adhesion between Graphene Family Materials (GFMs) and HA.

Moreover, to date, diverse mixing methods have been devised and implemented to enhance the homogeneous dispersion of Graphene Family Materials (GFMs) within the hydroxyapatite matrix by promoting potential electrostatic interactions between the surfaces of GFMs and hydroxyapatite (HA) (table 2). Several mechanical mixing techniques have been employed, including ultrasonication [77,78], ball milling [72,79], and mechanical stirring [80]. In addition to these mechanical methods, various chemical approaches have been explored, encompassing in situ precipitation [81], electrochemical deposition [82], andnotably, biomineralization [83,84]. Biomineralization stands out as a potent method to achieve a uniform dispersion of GFMs in the HA matrix, offering a straightforward approach to fabricate Graphene Family Materials-Hydroxyapatite (GFMs-HA) composites under mild conditions.

Biomimetic Mineralization of HA on GFMs

In general, biomineralization is a biological process by which living organisms produce minerals, typically in the form of crystals, within their tissues. This intricate process occurs in various organisms, including bacteria, plants, and animals, and plays a fundamental role in the formation and maintenance of skeletal structures, shells, teeth, and other mineralized tissues.for example biomineralization of hydroxyapatite (HA) is a fascinating biological process by which living organisms produce and regulate the formation of this calcium phosphate mineral within their tissues. The aim is to emulate these strategies and properties in the synthesis of synthetic inorganic materials [85-87].

Various theories have been formulated to elucidate the processes involved in crystal formation through nucleation and growth [88]. For instance, the classical theory posits that crystallization initiates through the association of initial clusters of ions or molecules, facilitated by collisions under supersaturation conditions [89]. The growth of crystals is further determined by either thermodynamic control or kinetic control [90,91] contingent upon the activation energy of nucleation, growth, and phase transformation. In

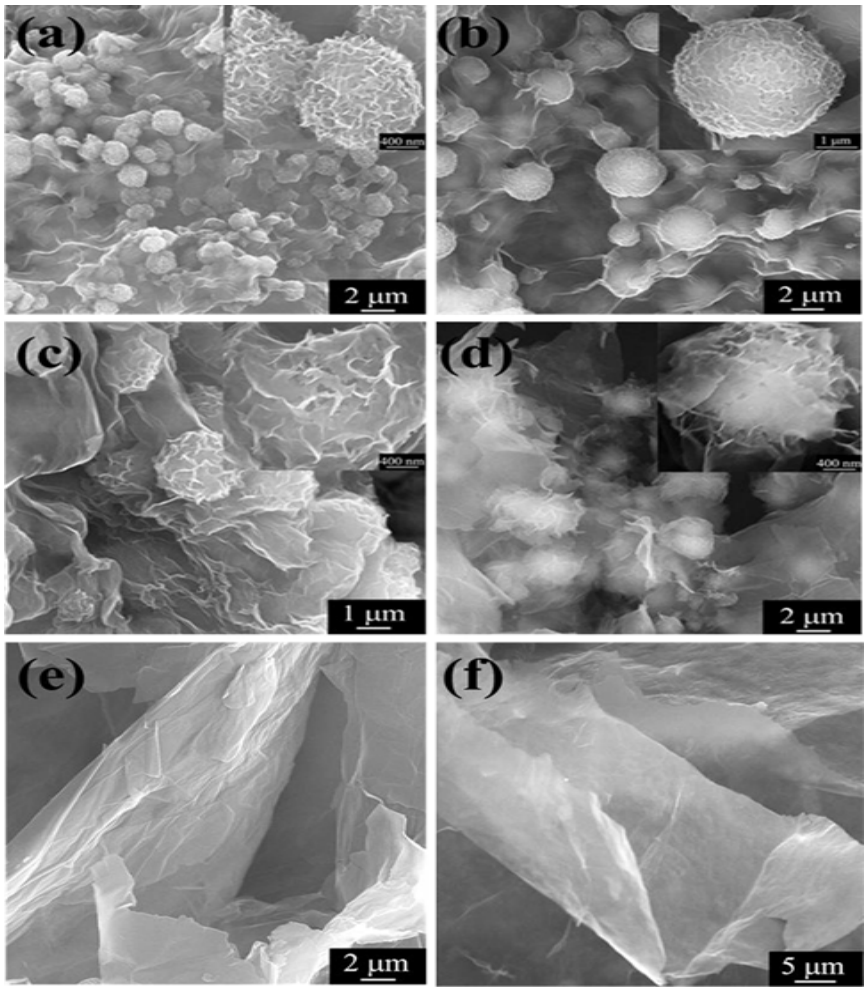

Figure 1: SEM images of GO–PNF nanohybrid after being soaked in 1.5 × SBF for (a) 1, (b) 3, (c) 7, and (d) 14 days. (e and f) SEM images of (e) pure GO and (f) GO after mineralization for 14 days [106]

Table 2: Mixing methods used to enhance the homogeneous dispersion of Graphene within the hydroxyapatite matrix

Nanocomposite	Mixing /dispersion method	dispersion State of HA in GFM, or GFM in HA	Reference
GO-chitosan-HA-	Solution Mechanical stirring/sonication	Appreciable aggregation of HA nanoparticles on the surface of chitosan-GO nanosheets	[103]
	in situ chemical precipitation	some aggregated HA at the edges of the sheets	[144]
	Solution Mechanical Agitation	Uniform dispersion of HA on the surface and the edges of GO-chitosan	[80]
	Solution mixing/ultrasonication	Uniform dispersion of HA on the surface and the edges of GO-chitosan	[78]
GO- sodium alginate – HA (10%, 20%,	Solution mixing/sonication	Uniform dispersion of HA on the surface for GO- sodium alginate –HA (10%, 20%), observable aggregation for GO- sodium alginate –HA (30%)	[172]
Three dimensional(3D) rGO-polypyrrole (PPY)	Biomimetic mineralisation	Uniform deposition of HA on the 3D rGO/PPY.	[84]
	Bio mimetic mineralisation	The surfaces of GO sheets were covered with HAP	[83]
	Ultrasonication	-Uniform dispersion of HA on GO surface ,and small number of them aggregated on the sheet edges	[79]
	electrochemical deposition on titanium(Ti) substrate	HA uniformly dispersed and attached onto GO sheets	[82]
	Ultrasonication	Homogeneous dispersion of Graphene in the porous composites.	[136]
	In situ precipitation	Homogeneous dispersion of Graphene in HA matrix	[81]
	Ball milling	No good dispersion of Graphene nanoplatelets	[79]
Graphene-Ni-doped HA	Mechanical mixing via planetary ball milling	Good dispersion of graphene nanoplatelets in the composite structure	[72]

thermodynamic control, the more stable phase is favored, while in kinetic control, crystallization proceeds through a series of phase transformations from less stable to more stable phases, in accordance with Ostwald's rule of stages [92].

An illustrative example of kinetic control in biomineralization is evident in the formation of dental calculus, where the crystallization of hydroxyapatite is regulated. Specifically, the process begins with the formation of the frequently less stable amorphous calcium phosphate (ACP) phase, followed by a sequential transformation to the more stable HA phase [93]. Moreover, organic molecules play a beneficial role in the formation of hydroxyapatite crystals during biomineralization processes by reducing the activation energy of nucleation and influencing the oriented morphology of the inorganic crystals formed [94,95].

In general, the biomineralization of HA can occur in the presence of two types of organic molecules: (i) soluble matrices, such as proteins and polysaccharides, and (ii) insoluble matrices, including graphene family materials (GFMs) and chitin.Particularly, graphene-family materials, as a form of insoluble matrix, exhibit attractiveness for the biomineralization of hydroxyapatite in simulated body fluid. This appeal is attributed to the functional groups present on the surface of GFMs, facilitating robust bonding to the nucleus. Furthermore, functionalizing GFMs becomes crucial to enhance the interaction between GFMs and ions in SBF. Consequently, amorphous calcium phosphate (ACP) and $CaHPO_4.2H_2O$, along with $Ca_4H(PO_4)_3$ and $Ca_{10}(PO)_6(OH)_2$, favor the nucleation and growth of HA on the support of GFMs. In contrast, inert materials lack the organic functional groups necessary for mineralization in SBF.

In recent years, numerous investigations have documented the biomineralization of hydroxyapatite on graphene family materials (GFMs), specifically graphene oxide, through the functionalization of GO with organic molecules such as polysaccharides, polymers, amino acids, and carboxylic acids. Leveraging potential electrostatic interactions between hydroxyapatite and GO or reduced graphene oxide, Liu et al. employed a straightforward method to create an rGO-HA composite. They functionalized GO through in situ polymerization of dopamine, leading to a polydopamine-coated rGO surface exhibiting nanoparticles of HA grains with a size of approximately 20 nm after 14 days of immersion in simulated body fluid (SBF) [96]. Li and colleagues adopted a biomimetic mineralization approach to prepare a GO-HA composite without functionalizing GO. In this method, HA exhibited accelerated growth within just 1 hour of incubation in SBF. After 8 hours, the HA crystals covered the entire surface of GO [83]. Núñez et al. also utilized the biomimetic mineralization method to synthesize a GO-HA composite. Bioactivity testing confirmed HA mineralization on the GO-HA surface after 7 days, as indicated by an increased Ca/P ratio from 1.41 to 1.48 [97]. Zhao et al. developed an rGO-silver nanoparticles (AgNPs) composite for mineralizing HA on its surface. Thioglycolic acid (TGA) was introduced to favor the nucleation of HA. After 5 days of incubation in SBF, HA growth was observed on the surface of rGO-AgNPs [98]. Additionally, a three-dimensional rGO/polypyrrole composite was mineralized using the electrodeposition method, resulting in uniform deposition of porous HA nanospheres with sizes ranging from 50 to 100 nm on the three-dimensional rGO/polypyrrole surface [84].

Furthermore, a three-dimensional GO-hydroxyapatite (GO-HAP) composite was synthesized in a modified SBF. Scanning electron microscopy (SEM) observations of GO incubated in SBF revealed crystal nucleation starting after 12 hours of incubation. After 3 days of incubation, a three-dimensional flower-like HA nanostructure was formed [99]. Similarly, graphene oxide (GO) has been subject to functionalization using gelatin [100], carrageenan [101] and chitosan [102,103], facilitating the mineralization of hydroxyapatite (HA). For instance, the surface of the GO-gelatin film exhibited spherical and porous aggregates of HA after a 14-day incubation in 1.5 simulated body fluid (SBF). This result can be attributed to the negatively charged carboxylic groups of gelatin, which attract ions, thereby promoting nucleation and growth of HA [100]. Additionally, the surface of the GO-carrageenan composite was initially covered with small irregular aggregates after 7 days of mineralization. However, after 14 days, the GO-carrageenan surface exhibited a uniform macroporous, spherical structure of HA [101].

Furthermore, a novel composite, GO-chitosan (Cs), designed for biomineralization, demonstrated a finely dispersed distribution of HA particles on its surface. This dispersion is attributed to the robust electrostatic interaction between ions in SBF and the carboxylic acid and amine groups on the surface of GO-Cs [102]. On the other hand, another category of biomolecules has been combined with graphene oxide (GO), such as amino acids and peptides, aiming to replicate the composition and structure of natural bone. For instance, GO was functionalized with arginine (Arg) or glutamic acid (Glu) via amidation reaction, after transforming all functional groups of GO into carboxylic acid. Arginine formed a stable complex exposing guanidyl and α-amino groups, facilitating bonding with Ca^{2+} and PO_4^{3-} in the simulated body fluid (SBF) solution. In comparison, Glutamic acid, which only exposed carboxylic groups, resulted in a slower precipitation of hydroxyapatite (HA) [104]. Additionally, the introduction of casein phosphopeptides (CsP) to GO expedited the formation of HA and reduced the time required for biomimetic mineralization. This acceleration was attributed to the negative charge of phosphorus groups, which strongly interacted with Ca^{2+} and PO_4^{3-} in the SBF solution [105]. Furthermore, for a comparative study on the short and long mineralization times of HA on GO composites, GO was combined with Peptide nanofibers (PNF). The GO-PNF composite, immersed in 1.5*SFB for 1 hour, 3 hours, and 1 day, demonstrated significantly faster biomimetic mineralization. Apatite crystals formed after just 1 hour, and after 3 hours, the spherical apatite structures were comparable in size and structure to those formed after 1 day (figure 1) [106].To further confirm the rapid mineralization of HA on GO, a three-dimensional nanocomposite, GO-fibrinogen nanofibers (FNf), was prepared using a layer-by-layer assembly method on a silicon support. Upon immersion in 1.5*SFB, AFM analysis confirmed that HA mineralization occurred after 1 hour, and SEM imaging revealed uniform decoration of the GO-FNf surface with branch-like apatite structures after 7 days of mineralization [107].

Recently, numerous researchers have proposed potential mechanisms for the biomimetic mineralization of hydroxyapatite (HA) in the presence of graphene family materials (GFMs) [83,99,108]. However, these proposed mechanisms have primarily focused on the role of organic functional groups in promoting biomimetic mineralization, often overlooking the influence of kinetic and thermodynamic controls. In our review, we present a straightforward mechanism to elucidate the biomimetic mineralization of HA on GFMs, considering the potential involvement of thermodynamic and kinetic controls in governing the formation of HA crystals.

The polar functional groups present on the surface of GFMs serve as nucleation and growth sites for HA. Initially, positively charged calcium ions (Ca^{2+}) exhibit a strong electrostatic interaction with the negatively charged functional groups on the GFM surface,

leading to the adsorption of calcium ions onto the GFMs. Subsequently, phosphate ions (PO_4^{3-}) adsorb onto the GFM-Ca^{2+} surface, forming GFM-Ca^{2+}-PO_4^{3-}. Following this interaction, the spontaneous nucleation and growth of HA commence, resulting in the eventual formation of HA crystals after an extended incubation period in simulated body fluid (SBF). Depending on the prevailing conditions, HA crystals may form directly under thermodynamic control or indirectly through a sequential transformation from a less stable phase to HA under kinetic control.

Toxicity, proliferation, differentiation, adhesion of cell on GFMs-HA

The toxicity, proliferation, differentiation, and adhesion of cells on graphene-hydroxyapatite (GHA) composite materials are critical considerations in assessing their biocompatibility and suitability for biomedical applications. Understanding how cells interact with GHA composites is essential for evaluating their potential for use in tissue engineering, regenerative medicine, and biomedical implants.

The demand for novel composite materials to enhance fracture repair, treat fractures, and stimulate bone formation has intensified. However, it is imperative to gain insights into the interactions between biomaterials and cells to develop materials that can expedite the adhesion, growth, and osteogenic differentiation of bone cells. Cellular behavior is significantly influenced by the physicochemical properties of the biomaterial surface. Additionally, surface roughness, reactivity, and chemical composition play crucial roles in mediating the interaction between cells and biomaterials [109–111]. For instance, the capacity of graphene family materials (GFMs) to accelerate cell growth and differentiation stems from molecular interactions between the functional groups on their surfaces and cellular proteins through covalent, electrostatic, and hydrogen bonding. Furthermore, favorable surface properties such as thickness and roughness create an environment conducive to cell differentiation and proliferation [87,112,113].

Recently, graphene family materials (GFMs) have garnered significant attention in the context of stem cell culture due to their potential to enhance the proliferation and differentiation of various cell types, including mesenchymal stem cells, [114–116] and neural stem cells [117-120]. However, ensuring the non-toxicity of GFMs is crucial for their potential applications in bone regeneration. Several studies have reported that GFMs exhibit no apparent cytotoxicity at lower concentrations [121,122]. Nevertheless, the toxicity is contingent on factors such as shape, size, purity, post-production processing steps, oxidative state, functional groups, dispersion state, synthesis method route, dose of administration, and exposure time of graphene and its derivatives [123]. On the other hand, hydroxyapatite is a bioactive biomaterial known for its ability to stimulate the differentiation of osteoblastic cells. However, its capacity to stimulate the proliferation and differentiation of osteoblastic cells is comparatively lower than that of other bone substitutes [124,125]. Adding another layer of complexity, understanding the impact of introducing GFMs to hydroxyapatite raises questions about whether they can further enhance cell differentiation and proliferation or not.

Recently, a growing body of research has demonstrated that the incorporation of graphene family materials (GFMs) into hydroxyapatite (HA) can positively influence cellular behavior, leading to increased proliferation and differentiation. Cells exhibit enhanced adhesion to GFMs-HA compared to HA alone, and the addition of GFMs mitigates cytotoxicity, as summarized in Table 3. For instance, cellular growth was unaffected at concentrations as high as 10 μg/ml of rGO-HA nanocomposite, whereas HA alone exhibited a decrease in cellular viability at 31.3 μg/ml. Moreover, cellular proliferation was not adversely affected by the composite, and the incorporation of rGO into HA stimulated higher alkaline phosphatase (ALP) activity. Additionally, rGO-HA nanocomposite demonstrated a higher deposition of calcium on MC3T3-E1 cells compared to both HA and rGO [126].

Furthermore, cellular growth on GFMs-HA composite remained uninhibited even at concentrations below 31.3 μg/ml, and cellular proliferation was not adversely affected when cells were cultured with a 10 μg/ml composite. The synergistic effect of HA and rGO led to enhanced calcium deposition in MC3T3-E1 cells. Notably, the rGO-HA composite exhibited a significant increase in the expression levels of osteopontin (OPN) and osteocalcin (OCN)

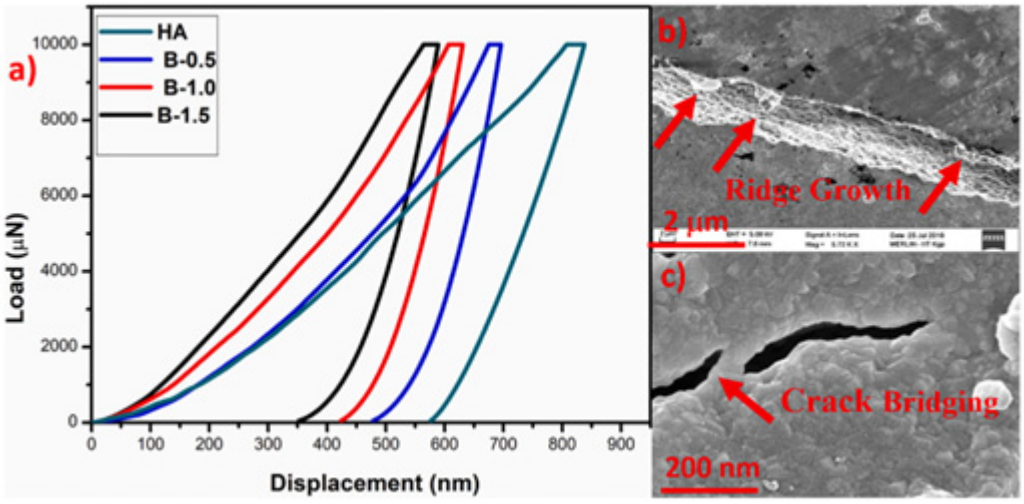

Figure 2 : (a) Load vs displacement curves of HA and nanocomposites, FESEM analysis showing crack inhibition by b) ridge growth, c) crack-bridging by grphene sheets [132]

Table 3: Toxicity, proliferation, differentiation, adhesion of cell on GFMs-HA

Composite	Concentration or % of GFM on HA	Cytotoxicity assay	Cell proliferation and adhesion assay	Cells type
rGO/HA	-	Insignificant cytotoxicity at 10µg/mL.	not promote the adhesion and proliferation of the cells	A murine preosteoblastic cell line (MC3T3-E1 preosteoblasts from C57BL/6 mouse calvaria)
rGO/HA	-	Any significant toxicity at lower concentration than 31.3µg/ml, IC50=1091 µg/ml	The cellular proliferation not adversely affected by rGO/HA	
Graphene nanosheet-HA	40,60 and 80 wt%	Higher cells viability at 60 wt% of GO	Promote High adhesion and proliferation of the cells at 60 wt% of GO	
Gelatine-GO-HA	-	Enhance the cells viability	Promote adhesion and proliferation of the cells	
rGO-HA	-	Any significant toxicity at lower concentration than 62.5 µg/ml, IC50 = 737 µg/ml	Promote proliferation of the cells	hMSCs
Gold/Hydroxy-apatite/graphene	1.60, 3.15, 5.10, and 7.34 wt%	Highest number of cells at 30 µg/ml of Au/HA/Gr (13.15 wt %)	-	-
Silk fibroin-GO-HA	-	Any significant toxicity	Good proliferation after day 4	Human osteoblast-like cell (MG63)
rGO/HA	0.5, 1.0 and 1.5 wt%	Excellent biocompatibility at 1.5 wt% of rGO	Promote High adhesion and proliferation of the cells at 1.5 wt% of rGO	Human osteoblast cell lines (HFOB 1.19 SV40 transfected osteoblasts)
Graphene nanoplatelets/HA doped Ni (6 %)	0.5, 1.0, 1.5, and 2 wt%	-		
Graphene nanosheet-HA	0.1 and 1 wt%	High cell viability at 1wt% of GNS	High cell proliferation at 1 wt% of graphene	
rGO/HA	40 wt%	high cell viability	-	Mouse multipotent mesenchymal stromal cells (MSCs; also known as mesenchymal stem cells)
3D (GO–fibrinogen nanofibers)10HA	-	Excellent cytocompatibility	High proliferation ability	fibroblast cell line L-929
rGO/HA	-	-	promote the adhesion and proliferation of the cells	Bone marrow- derived stem cells (rBMSCs)
Chitosan-GO-HA	-	high cell viability		
GO-coated porcine bone	50, 100 µg/ml	Not exert cytotoxic effect on HGF	-	Human gingival fibroblasts (HGF)
Fibrin –GO-HA	-	high cell viability rate	-	MG-63 cells
Chitosan-GO-HA	1, 1.7 wt%	Acceptable cytotoxicity at 1.7wt% of GO	-	MG63 cells
Chitosan-GO-HA GO–HA	-	Excellent in vitro cytocompatibility within a concentration of 100 µg/ml .	-	the murine fibroblast L-929 cell line and human

proteins in MC3T3-E1 cells [127]. In a separate study, rGO-HA composite concentrations up to 62.5 µg/ml did not induce cytotoxic effects, and cellular proliferation remained unaffected. After 14 days, the cells exhibited significantly higher ALP activity, and the expression levels of OPN and OCN proteins were markedly increased after 21 days [128]. Additionally, GO-coated porcine bone at concentrations of 50 and 100 µg/ml of GO did not demonstrate a significant cytotoxic effect on Human Gingival Fibroblasts (HGF) cells [129]. Also, In vitro cytocompatibility assessments demonstrate that nanorod hydroxyapatite/graphene oxide composites NRHA/GO composites support cell adhesion and growth, suggesting their potential as non-toxic, bioactive materials for bone tissue repair and regeneration [130]. In addition to this, in vitro cell-graphene nanosheets on the plasma sprayed hydroxyapatite coating interaction studies with MG-63 cells reveal enhanced biocompatibility of the GNS/HA composite coating. This is evidenced by improved cell attachment, adhesion strength, proliferation, and differentiation. These findings suggest the potential of GNS/HA composite coatings for biomedical applications, particularly in enhancing osteoblast performance and promoting bone regeneration [131]. Furthermore, in vitro studies of green synthesized graphene-hydroxyapatite nanocomposites demonstrate promising results, with the nanocomposites exhibiting 140% cell viability for human embryonickidney cells at a concentration of 200 µg/mL. Additionally, they demonstrate osteoconductivity in simulated body fluid solution [132]. Moreover, the graphene-hydroxyapatite nanocomposites exhibited 100% viability of HEK 293 cells at a concentration of 12.5 µg/mL and demonstrated in vitro apatite mineralization when immersed in simulated body fluid (SBF) solution for 7 days. These findings

Table 3 (cont.): Toxicity, proliferation, differentiation, adhesion of cell on GFMs-HA

Osteogenesis examination by ALP activity assay	Osteogenesis examination by Von Kossa staining	Western blotting	Alizarin red S (ARS) Staining	Reference
Increasing of ALP activity after 14 days	Osteogenic differentiation of MC3T3-E1 preosteoblasts on day 28	Increasing of OCN level in MC3T3-E1 preosteoblasts on day 21	Formation of calcium from 14 to 21 days.	[126]
Significant increase of ALP activity from 14 to 21 day	Significant osteodifferent ation of MC3T3-E1 preosteoblasts on day 28 at 10 µg /mL.	Significant increase on OCN, and OPN level in MC3T3-E1 preosteoblasts on day 21	Significant increase of calcium deposition between 14 and 21 day	[127]
-	-	-	-	[134]
-	-	-	-	[145]
Significantly higher ALP activity after 14 days	significantly induced osteoblast differentiation with the formation of mineralized nodules by hMSCs	After 21 days of incubatio, expression levels of both proteins in hMSCs were significantly ($p < 0.05$) increased by rGO-coated HAp composites.	a notable formation of calcium deposits from 14 to 21 days	[128]
-	-	-	-	[137]
No significant differences in ALP activities	-	-	-	[147]
-	-	-	-	[135]
-	-	-	-	[72]
Increase ALP activitie of composite at 1 wt% two times more than HA	-	-	-	[81]
-	-	-	-	[136]
-	-	-	-	[107]
-	-	-	-	[170]
-	-	-	-	[80]
-	-	-	-	[129]
High ALP activity at 50 µg/ml, 100µg/ml of composite and decrease of ALP activity after 12 day at 100µg/ml	-	-	-	[146]
-	-	-	-	[78]
higher ALP activities have been obtained for the MG-63	-	-	-	[144]

underscore the potential of RGO-HA nanocomposites as promising materials for bone implant applications [133].

On the other hand, the variation in GFMs concentration has a positive impact on cellular behavior within the GFM-HA composite. For instance, Graphene Nano Sheet (GNS)-HA at a concentration of 60 wt% GNS exhibited the highest cell viability and robust proliferation compared to composites with 40% and 80% GNS. Notably, cells adhered to the surface of HA-GNS (60 wt%) with a fusiform structure and microscopic filopodia [134]. In the case of sintered HA-rGO nanocomposite, a concentration of 1.5 wt% rGO demonstrated superior proliferation and excellent biocompatibility with human fetal osteoblastic cells (hFOB 1.19) compared to other concentrations (0%, 0.5%, and 1 wt%) [135]. Additionally, the addition of 1.5% GNS to HA doped with Nickel positively influenced cell viability and proliferation of hFOB [72]. Furthermore, a gel nanocomposite of rGO-HA at 40 wt% rGO exhibited high cell viability with mesenchymal stem cells. The cells adhered to the nanocomposite surface with elongated fine filamentous structures, attributed to the porous structure of the nanocomposite [119,136]. In the case of HA-GNS at 1% GNS, the highest cell viability, proliferation, and ALP activity were observed compared to HA alone and HA-GNS (0.1 wt%). The biological activity demonstrated a correlation with GNS concentration, indicating an increase in the number of cells with higher GNS concentration [81]. Moreover, Gold/Hydroxyapatite/graphene at a concentration of 3.15 wt % graphene exhibited the highest number of osteoblast cells at 30 ig/ml of the nanocomposite compared to other concentrations (1.6%, 5.10%, 7.34 wt%). The most favorable proliferation and adhesion of cells

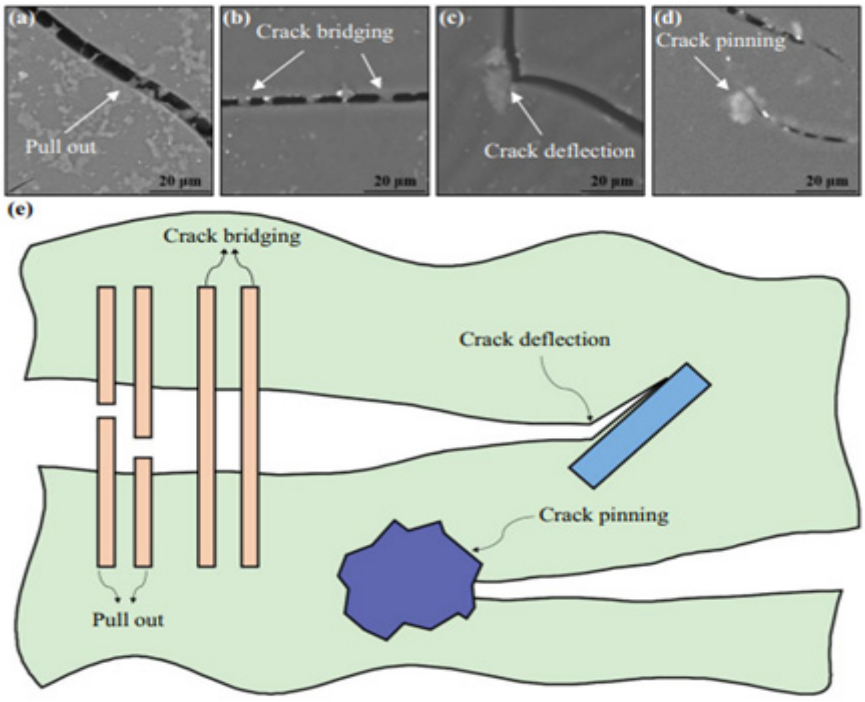

Figure 3: SEM images of crack propagation in the PLLA/GO-HAP scaffolds including pull out (a), crack bridging (b), crack deflection (c), crack pinning (d), and the corresponding crack extension model (e) [154]

were observed for the nanocomposite at 1.6% and 3.15% graphene [137]. Cytotoxicity assays of Nanocomposite powders of hydroxyapatite-graphene oxide for biological applications reveal that despite a decrease in the viability and proliferation of human dental pulp stem cells (hDPSCs) with increasing GO concentration up to 1.5 wt%, HA-GO nanocomposites still exhibit high levels of cell viability [138].

Moreover, the functionalization of graphene oxide with organic molecules such as chitosan, gelatin, fibrin, fibrinogen, and silk fibroin has been demonstrated to positively influence the cellular behavior of GFMs-HA nanocomposites. The presence of these molecules creates a favorable microenvironment for cell differentiation, proliferation, and the formation of mineralized tissue [139–143]. For instance, MG-63 cells exhibited significantly higher alkaline phosphatase (ALP) activity on Chitosan-GO–HA composite compared to GO–HA composite. The viability of cells increased from 80% to 100% and 110% for GO–HA and CS-GO–HA, respectively, over time [144]. Similarly, rBMSCs cells demonstrated high cell viability and robust proliferation on Chitosan-GO-HA surfaces [80]. Gelatin-GO-HA enhanced the proliferation and adhesion of preosteoblastic cells (MC3T3-E1), with the cells exhibiting a fusiform structure strongly binding with filopodia to the composite surface [145]. Furthermore, Fibrin-GO-HA exhibited a high cell viability rate and elevated ALP activity compared to GO and GO-HA. Notably, Fibrin-GO-HA demonstrated significant calcium deposition on MG-63 cells at concentrations of 50 and 100 μg/ml, outperforming GO and GO-HA [146]. The fibroblast cell line L-929 exhibited excellent cytocompatibility and proliferation on three-dimensional GO–fibrinogen nanofibers–HA, with no dead cells observed [107]. Additionally, silk fibroin (SF)-GO-HA showed a good proliferation rate, around or above 75%, on Human osteoblast-like cells (MG63), with no significant differences in ALP activities. This observation is attributed to the low content of HA and GO in this composite [147]. Moreover, in vivo experiments utilizing a distal femoral condyle critical size defect model in rabbits confirm the positive effect of N doped Graphene "Hydroxyapatite/Agarose AG/NG" HA hybrid scaffolds on bone regeneration. Cell experiments further demonstrate that AG/NG HA nanocomposites support cell adhesion, proliferation, and osteogenic gene expression, leading to osteogenic differentiation. significantly promoting osteogenesis and the repair of bone defects in vivo [148]. Furthermore,the three-dimensional scaffold composed of reduced graphene oxide/polyurethane 3DrGO/PU scaffold demonstrated excellent support for the growth and proliferation of mouse osteoblast cells (MG-63), exhibiting strong mineralization and cell attachment. This is attributed to the scaffold's electrically conductive macro-porous structure, which likely promotes the nucleation and growth of hydroxyapatite (HA) in simulated body fluid [149], in addition.

Mechanical Properties of GFMs-HA

The mechanical properties of hydroxyapatite-graphene composite materials are of significant interest due to their potential applications in various fields, including biomedical engineering, materials science, and structural engineering. These properties are influenced by the composition, microstructure, and processing techniques employed in fabricating the composite materials. Hydroxyapatite (HA) is known for its excellent biocompatibility and similarity to the mineral phase of natural bone, making it a promising material for orthopedic implants, bone substitutes, and tissue engineering scaffolds. However, pure HA lacks sufficient mechanical strength and toughness for load-bearing applications, which has led to research efforts to enhance its mechanical properties through composite formation.

Enhancing the mechanical properties of hydroxyapatite (HA) is currently in high demand to address the inherent brittleness associated with HA. Dense HA exhibits superior mechanical characteristics, including elastic modulus, compressive strength, and tensile strength, compared to natural bone and porous HA. This can be attributed to its higher density, absence of microporosity, and interconnected macroporosity. However, both dense and porous HA exhibit limitations in terms of fracture toughness, restricting their biomedical applications. To overcome this challenge, it is prudent to reinforce HA with a secondary matrix that can effectively impede the propagation of cracks. Graphene, a two-dimensional carbon allotrope with exceptional mechanical properties, such as high tensile strength, stiffness, and toughness, has emerged as a promising reinforcement material for enhancing the mechanical properties of HA composites. Incorporating graphene into HA matrices can improve the composite's mechanical strength, fracture resistance, and fatigue performance, while maintaining its biocompatibility and bioactivity.

Recently, graphene-family materials (GFMs) have emerged as compelling candidates for reinforcing hydroxyapatite (HA) to enhance its fracture toughness. For instance, incorporating 1% graphene nanosheet (GNS) through the vacuum cold spray (VCS) process resulted in a remarkable 280% increase in fracture toughness compared to pure HA [150]. Similarly, HA-GNS composites prepared via VCS demonstrated an escalating trend in fracture toughness (KIC) with increasing GNS content, reaching 0.421 ± 0.011 MPa at 1% GNS [81]. Furthermore, the fracture toughness of HA-reduced graphite oxide (rGO), consisting of 2–6 layers of graphene and prepared by precipitation followed by spark plasma sintering (SPS) consolidation, exhibited a notable 203% improvement compared to pure HA. Additionally, the elastic modulus and hardness increased by 47.6% and 25.8%, respectively [151]. In another study, HA-GNS with 1% GNS, synthesized using SPS, demonstrated an 80% enhancement in fracture toughness compared to pure HA. This improvement is attributed to the presence of graphene, which deflects crack propagation or hinders crack growth [152]. Moreover, biphasic calcium phosphate (BCP), a composite of HA and beta-tricalcium phosphate, was reinforced with graphene. BCP-graphene with 1.5% graphene content exhibited the highest fracture toughness and bending strength, surpassing those of BCP alone by approximately 76% and 55%, respectively.

On the other hand the incorporation of graphene oxide (GO) into polylactic acid/hydroxyapatite (PLA/HA) composites led to notable enhancements in tensile strength and hardness. As the content of GO increased, both tensile strength and hardness of the PLA/HA/GO composites showed a corresponding increase. This enhancement in mechanical properties can be attributed to the increased hardness of the PLA/HA/GO composites resulting from the higher content of GO, thereby endowing the composite with extraordinary mechanical characteristics [153]. Furthermore, mechanical properties of green-synthesized graphene-hydroxyapatite (HA) nanocomposites assessed through nanoindentation and vicker indentation techniques reveal significant enhancements in elastic modulus, microhardness, and fracture toughness values by 114%, 36%, and 141%, respectively. Moreover, roughness and coefficient of friction values experience enhancements of 110% and 40%, respectively, in these nanocomposites (figure 2) [132]. Likewise, the study focuses on the in situ synthesis of hydroxyapatite nanorods on graphene oxide nanosheets and their reinforcement in a biopolymer scaffold. Results show that the compressive strength and modulus of the PLLA/12%GO-HAP composite were significantly increased by 53.71% and 98.80%, respectively, compared to the pure Poly-L-Lactic Acid (PLLA) scaffold. This enhancement is attributed to mechanisms such as pull out (figure 3) [154]. The study focuses on the fabrication of a zirconia/reduced graphene oxide/hydroxyapatite (ZrO_2/RGO/HA) scaffold using a rapid prototyping method and investigates its mechanical and biocompatibility properties. Results from compression testing revealed that the addition of 2%wt. of RGO as reinforcement in the ZrO_2/HA matrix exhibited desirable behavior, enhancing the mechanical properties of the scaffold [155].

In addition, the hydroxyapatite/chromium oxide/graphene oxide ($HAP/Cr_2O_3/GO$) nanocomposite exhibits the highest microhardness, measuring at 3.7 ± 0.3 GPa. This enhancement is

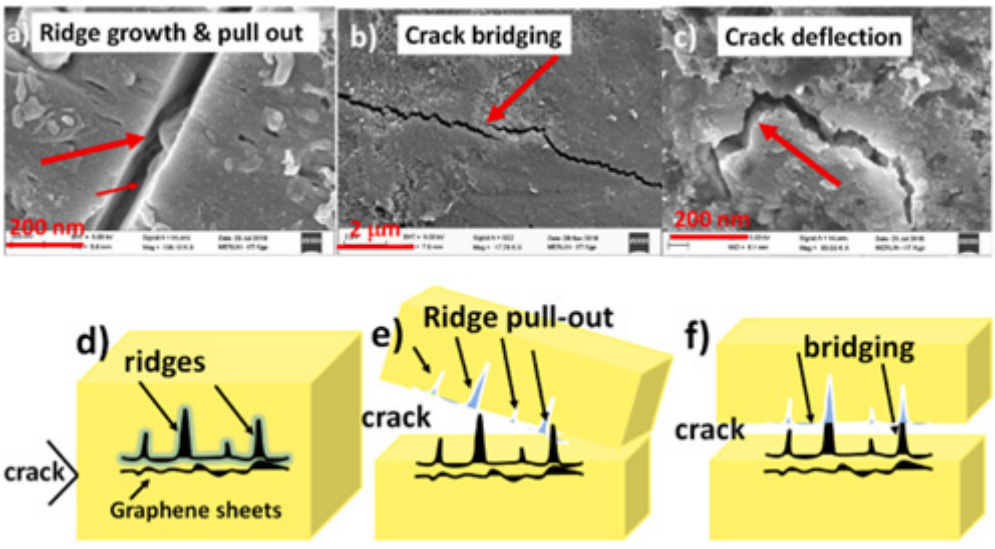

Figure 4: FE-SEM images showing a) radially propagating cracks and ridge growth (pointed by long arrows), inhibition of crack propagation with graphene sheets b) through crack-bridging c) crack deflection, graphical illustrations of d) ridges e) ridge pull-out, and f) bridging by RGO in HA matrix [133]

attributed to the efficient load transfer mechanism facilitated by the good interfacial bonding formed between GO and other components [156]. Another study focuses on optimizing the fabrication process and characterizing the mechanical properties of 3D-printed hydroxyapatite/gelatin bone scaffolds reinforced with graphene oxide (GO) demonstrate that the addition of GO effectively enhances the mechanical properties of the HA/gelatin composite scaffolds. Specifically, the incorporation of 0.5% GO leads to a 15% increase in compressive strength and a 22% increase in flexural strength compared to scaffolds without GO reinforcement [157].

Also thegraphene-hydroxyapatite (RGO-HA) nanocomposites demonstrated notable enhancements in the mechanical properties of RGO-HA nanocomposites. Specifically, the elastic modulus, microhardness, and fracture toughness values increased by 100%, 33.3%, and 64.5%, respectively, with the addition of 1.5 wt% graphene in the HA matrix [133]. Also reduced graphene oxide (HA-rGO) through chemical synthesis, compared to calcined hydroxyapatite (cHAp), showed that the strength of variants significantly increased with higher concentrations of rGO. The compressive strength of HA-rGO with a weight ratio of 60:40% reached a maximum of approximately 10.39 ± 0.43 MPa [158]. Furthermore the nanocomposite scaffolds based on polyvinyl alcohol-chitosan containing hydroxyapatite and clay modified with graphene oxide exhibited a compressive strength of 9.31 MPa [159].

Moreover, results indicate that the GNS/HA composite coating exhibits improved strength and toughness compared to plasma-sprayed HA coating. There is a significant increase in fracture toughness (~32.3%) and indentation yield strength (~54.7%) in the composite coating. This enhancement is attributed to synergistic toughening and strengthening mechanisms, including load transfer, GNS pull-out, inter-layer sliding of GNS, crack branching, and GNS bridging. Moreover, frequent crack deflection upon contact with GNS contributes to tailoring the trade-off between strength and toughness by resisting or extending crack propagation [131].

Various toughening mechanisms contribute to the increased fracture toughness of hydroxyapatite (HA) in composite materials. These mechanisms, observed during composite fracturing, include crack deflection, crack branching, crack bridging, and pull-out mechanisms. load transfer, and inter-layer sliding These toughening mechanisms arise from the interplay between crack propagation and the presence of graphene-family materials (GFMs), and similar observations have been made in ceramic materials [131,160–164].

Crack bridging

Crack bridging in graphene refers to a phenomenon where cracks or defects within the graphene lattice are spanned or filled in by other materials, such as polymers or nanoparticles. This process serves to enhance the mechanical strength and resilience of graphene-based materials by preventing crack propagation and failure. Essentially, when cracks form in the graphene structure, adjacent materials bridge across the gaps, providing support and preventing the crack from spreading further (figure 4).

Crack deflection

Crack deflection in graphene occurs when a crack encounters the graphene lattice and changes its propagation direction. This phenomenon is a result of the exceptional mechanical properties of graphene, including its high strength and stiffness. When a crack approaches a graphene sheet, the strong covalent bonds between carbon atoms in the graphene lattice can act as barriers, causing the crack to deviate from its original path. As a result, the crack may change direction, deflecting along the graphene surface instead of propagating directly through it [162,163].

Pull-out mechanism

In the pull-out mechanism, some or all of the graphene sheets are pulled out of the matrix material, leaving voids or gaps behind. This process helps to dissipate energy and prevent catastrophic failure by redistributing stress within the composite material. Additionally, the pull-out of graphene sheets can enhance the toughness and fracture resistance of the composite by promoting crack deflection and bridging (figure 4) [152].

Crack branching

Crack branching in graphene occurs when cracks propagate in multiple directions within the graphene lattice structure This phenomenon often arises due to the unique mechanical properties of graphene, such as its exceptional strength and flexibility. When subjected to mechanical stress or deformation, cracks may initiate and propagate along certain planes or directions within the graphene sheet [165].

Load transfer

Load transfer in graphene refers to the process by which mechanical loads, such as stress or strain, are efficiently transferred between graphene and its surrounding materials or structures. When subjected to mechanical loading, the graphene sheets within the composite experience stress or strain. Efficient load transfer ensures that these mechanical forces are effectively transmitted from the matrix material to the graphene reinforcement, and vice versa. This allows graphene to contribute to the overall mechanical performance of the composite by bearing a significant portion of the applied load.

Interlayer sliding

Interlayer sliding in graphene refers to the ability of individual graphene layers to slide or shear relative to each other within a stacked configuration. Graphene, being a two-dimensional material, can be layered to form multilayer graphene structures. In these structures, adjacent graphene layers are held together by weak van der Waals forces. Interlayer sliding occurs when the interlayer van der Waals interactions are overcome by an external force or stress, allowing the graphene layers to slide past each other. This sliding motion can result in changes in the overall shape or configuration of the multilayer graphene structure.

The mechanical properties of hydroxyapatite-graphene-family materials (HA-GFMs) are influenced by the synthesis process parameters. For instance, the HA-GNS (2%) produced through Spark Plasma Sintering (SPS) at a sintering temperature of 700°C for 5 minutes exhibited the highest bending strength and hardness.[164] In the case of HA-rGO, prepared using a hydrothermal method followed by consolidation at 1150°C and 160 MPa, the elastic modulus and fracture toughness increased by 86% and 40%, respectively, with an increase in rGO concentration. This enhancement is attributed to the homogeneous dispersion of rGO within the HA matrix and the strong interaction between the two matrices [135]. Furthermore, the relative density serves as a valuable parameter for understanding the variations in mechanical properties in HA-GFMs. For instance, Bajpai et al. measured the relative density of HA-GNSs at 3% and 5% GNS concentrations, sintered at temperatures of 900°C, 1000°C, and 1100°C. All HA-GNS composites exhibited lower hardness than pure HA, indicating the impact of lower relative density in the HA-GNS composites [166].

On the contrary, orthopedic biomaterials play a crucial role in implants and accessories, encompassing metals, polymers, ceramics, or their composites. Metallic orthopedic biomaterials, particularly titanium and its alloys (Ti), are extensively employed for bone repair and regeneration. Titanium is often coated with hydroxyapatite (HA) to amalgamate the advantageous mechanical properties and high corrosion resistance of titanium with the biological properties of HA.

Complications such as cracks have been observed in HA-Ti coatings. To address these issues, it is imperative to control the porosity of biomaterials, thereby reducing the elastic modulus of HA-Ti [167]. Utilizing graphene-family materials (GFMs) at lower concentrations emerges as a viable solution to enhance adhesion strength and mitigate crack propagation in HA coatings on metallic substrates. For instance, Li et al. employed a cathodic electrophoretic deposition process (EPD) to fabricate a homogeneous GO-HAP nanocomposite on a titanium substrate (TiS). Compared to pure HA on TiS, GO-HA exhibited a notable absence of cracks or peeling. This was attributed to the presence of GO, which elevated the adhesion strength of HA from 1.55±0.39 MPa to 2.75±0.38 MPa and 3.3±0.25 MPa for HA-GO(2%) and HA-GO(5%), respectively [75]. Additionally, HA-Gr, prepared by EPD on TiS, demonstrated a twofold improvement in hardness compared to pure HA at an exceptionally low concentration of Gr (0.01%). [136, 168]. In another study by Zeng et al., investigating the adhesion strength between HA-GO and TiS via an electrochemical deposition technique, the adhesion strength increased with the concentration of GO [169].

Conclusions and Perspectives

In summary, this paper provides an overview of recent advancements in graphene family materials-hydroxyapatite composites. The review highlights the effectiveness of both chemical covalent and non-covalent functionalization methods, along with mechanical and chemical mixing techniques, in improving the dispersion of graphene family materials (GFMs) in both aqueous and organic solutions. These strategies result in excellent dispersion of GFMs within the hydroxyapatite (HA) matrix.

Furthermore, biomimetic mineralization emerges as a promising approach for constructing GFMs-HA composites due to its cost-effectiveness, low-temperature requirements, and short processing time. Additionally, functionalizing GFMs with organic or biomolecular agents enhances the mineralization of HA crystals on the surface of GFMs, thereby reducing mineralization time.

Studies have indicated that graphene family materials-hydroxyapatite (GFMs-HA) composites exhibit enhanced proliferation and differentiation of osteoblast cells compared to pure HA. Additionally, GFMs incorporated into HA promote stronger adhesion of osteoblasts to the composite surface than HA alone, with the biocompatibility of the composite being dependent on the GFMs content. Moreover, GFMs have been shown to reduce cracks in GFMs-HA composites by improving the fracture toughness of HA and increasing its elastic modulus and hardness. The mechanisms responsible for toughening include crack bridging, crack deflection, pull-out, a crack branching, load transfer, and inter-layer sliding.

However, it is important to note that research in this field is still in its early stages, and further investigation is required to fully explore the potential of GFMs-HA composites in bone regeneration. More relevant studies and efforts are needed to advance our understanding and utilization of GFMs-HA composites in this context.

The future research should encompass several key areas. Firstly, there is a pressing need to establish a standardized nomenclature for graphene family materials (GFMs) in research articles to ensure consistency and facilitate communication among researchers globally. Secondly, the potential of functionalizing GFMs with biocompatible molecules should be explored further, especially in biomimetic mineralization processes. The inclusion of polar functional groups on GFMs holds promise for enhancing mineralization and controlling the morphology of hydroxyapatite (HA) crystals. Moreover, efforts should be directed towards elucidating the interaction mechanisms between GFMs-HA composite surfaces and osteoblastic cells. This knowledge is crucial for developing GFMs-HA composites that can promote cell differentiation and proliferation without adverse effects. Additionally, thorough investigation into the long-term biocompatibility of GFMs-HA composites is essential before considering clinical applications. Lastly, there is a need for in-depth exploration of the toughening mechanisms of GFMs in both tridimensional and two-dimensional GFMs-HA composites. Understanding how GFMs contribute to increasing the fracture toughness of these composites will pave the way for enhancing their mechanical properties and expanding their potential applications.

References

1. S. Shinzato, M. Kobayashi, W.F. Mousa, M. Kamimura, M. Neo, Y. Kitamura, T. Kokubo, T. Nakamura, Bioactive polymethyl methacrylate-based bone cement: comparison of glass beads, apatite- and wollastonite-containing glass-ceramic, and hydroxyapatite fillers on mechanical and biological properties., J. Biomed. Mater. Res. 51 (2000) 258–272.
2. G.M. Calori, E. Mazza, M. Colombo, C. Ripamonti, The use of bone-graft substitutes in large bone defects: any specific needs?, Injury 42 Suppl 2 (2011) S56-63.
3. S.V. Dorozhkin, Bioceramics of calcium orthophosphates, Biomaterials 31 (2010) 1465–1485.
4. A.K. Geim, K.S. Novoselov, The rise of graphene, Nat. Mater. 6 (2007).
5. K.S. Novoselov, A.K. Geim, S.V. Morozov, D. Jiang, Y. Zhang, S.V. Dubonos, I.V. Grigorieva, A.A. Firsov, Electric field effect in atomically thin carbon films., Science 306 (2004) 666–669.
6. M. Kalbacova, A. Broz, J. Kong, M. Kalbac, Graphene substrates promote adherence of human osteoblasts and mesenchymal stromal cells, Carbon 48 (2010).
7. C. Lee, X. Wei, J.W. Kysar, J. Hone, Measurement of the elastic properties and intrinsic strength of monolayer graphene, Science 321 (2008).
8. M.D. Stoller, S. Park, Z. Yanwu, J. An, R.S. Ruoff, Graphene-Based ultracapacitors, Nano Lett. 8 (2008).
9. S. Cho, J. Jang, C. Song, H. Lee, P. Ganesan, T.Y. Yoon, M.W. Kim, M.C. Choi, H. Ihee, W.D. Heo, Y. Park, Simple super-resolution live-cell imaging based on diffusion-assisted Förster resonance energy transfer, Sci. Rep. 3 (2013).
10. L. Feng, L. Wu, X. Qu, New horizons for diagnostics and therapeutic applications of graphene and graphene oxide, Adv. Mater. 25 (2013).
11. C. Heo, J. Yoo, S. Lee, A. Jo, S. Jung, H. Yoo, Y.H. Lee, M. Suh, The control of neural cell-to-cell interactions through non-contact electrical field stimulation using graphene electrodes, Biomaterials 32 (2011).
12. W. Hu, C. Peng, W. Luo, M. Lv, X. Li, D. Li, Q. Huang, C. Fan, Graphene-based antibacterial paper, ACS Nano 4 (2010) 4317–4323.
13. J.L. Li, B. Tang, B. Yuan, L. Sun, X.G. Wang, A review of optical imaging and therapy using nanosized graphene and graphene oxide, Biomaterials 34 (2013).
14. X. Sun, Z. Liu, K. Welsher, J.T. Robinson, A. Goodwin, S. Zaric, H. Dai, Nano-graphene oxide for cellular imaging and drug delivery, Nano Res. 1 (2008) 203–212.
15. L. Zhang, J. Xia, Q. Zhao, L. Liu, Z. Zhang, Functional graphene oxide as a nanocarrier for controlled loading and targeted delivery of mixed anticancer drugs, Small 6 (2010).
16. Y. Zhang, T.R. Nayak, H. Hong, W. Cai, Graphene: A versatile nanoplatform for biomedical applications, Nanoscale 4 (2012) 3833–3842.
17. V.C. Sanchez, A. Jachak, R.H. Hurt, A.B. Kane, Biological interactions of graphene-family nanomaterials: An interdisciplinary review, Chem. Res. Toxicol. 25 (2012).
18. P. Wick, A.E. Louw-Gaume, M. Kucki, H.F. Krug, K. Kostarelos, B. Fadeel, K.A. Dawson, A. Salvati, E. Vázquez, L. Ballerini, M. Tretiach, F.

Benfenati, E. Flahaut, L. Gauthier, M. Prato, A. Bianco, Classification framework for graphene-based materials, Angew. Chem. - Int. Ed. 53 (2014).
19. W. DEHEER, C. BERGER, X. WU, P. FIRST, E. CONRAD, X. LI, T. LI, M. SPRINKLE, J. HASS, M. SADOWSKI, ScienceDirect - Solid State Communications/: Epitaxial graphene, Solid State Commun. 143 (2007).
20. X. Li, W. Cai, J. An, S. Kim, J. Nah, D. Yang, R. Piner, A. Velamakanni, I. Jung, E. Tutuc, S.K. Banerjee, L. Colombo, R.S. Ruoff, Large-area synthesis of high-quality and uniform graphene films on copper foils, Science 324 (2009).
21. M. Lotya, Y. Hernandez, P.J. King, R.J. Smith, V. Nicolosi, L.S. Karlsson, F.M. Blighe, S. De, Z. Wang, I.T. McGovern, G.S. Duesberg, J.N. Coleman, Liquid Phase Production of Graphene by Exfoliation of Graphite in Surfactant/Water Solutions, J. Am. Chem. Soc. 131 (2009) 3611–3620.
22. E. Ou, Y. Xie, C. Peng, Y. Song, H. Peng, Y. Xiong, W. Xu, High concentration and stable few-layer graphene dispersions prepared by the exfoliation of graphite in different organic solvents, RSC Adv. 3 (2013).
23. E. Rollings, G.H. Gweon, S.Y. Zhou, B.S. Mun, J.L. McChesney, B.S. Hussain, A.V. Fedorov, P.N. First, W.A. de Heer, A. Lanzara, Synthesis and characterization of atomically thin graphite films on a silicon carbide substrate, J. Phys. Chem. Solids 67 (2006).
24. G. Wang, J. Yang, J. Park, X. Gou, B. Wang, H. Liu, J. Yao, Facile Synthesis and Characterization of Graphene Nanosheets, J. Phys. Chem. C 112 (2008) 8192–8195.
25. S. Yang, M.R. Lohe, K. Müllen, X. Feng, New-Generation Graphene from Electrochemical Approaches: Production and Applications, Adv. Mater. 28 (2016).
26. Y. Zhu, M.D. Stoller, W. Cai, A. Velamakanni, R.D. Piner, D. Chen, R.S. Ruoff, Exfoliation of graphite oxide in propylene carbonate and thermal reduction of the resulting graphene oxide platelets, in: 2010.
27. W.S. Hummers, R.E. Offeman, Preparation of Graphitic Oxide, J. Am. Chem. Soc. 80 (1958). https://doi.org/10.1021/ja01539a017.
28. M.C. Kim, G.S. Hwang, R.S. Ruoff, Epoxide reduction with hydrazine on graphene: A first principles study, J. Chem. Phys. 131 (2009).
29. H.J. Shin, K.K. Kim, A. Benayad, S.M. Yoon, H.K. Park, I.S. Jung, M.H. Jin, H.K. Jeong, J.M. Kim, J.Y. Choi, Y.H. Lee, Efficient reduction of graphite oxide by sodium borohydride and its effect on electrical conductance, Adv. Funct. Mater. 19 (2009).
30. S. Stankovich, D.A. Dikin, R.D. Piner, K.A. Kohlhaas, A. Kleinhammes, Y. Jia, Y. Wu, S.B.T. Nguyen, R.S. Ruoff, Synthesis of graphene-based nanosheets via chemical reduction of exfoliated graphite oxide, Carbon 45 (2007).
31. S. Thakur, N. Karak, Alternative methods and nature-based reagents for the reduction of graphene oxide: A review, Carbon 94 (2015).
32. D. Had•i, A. Novak, Infra-red spectra of graphitic oxide, Trans. Faraday Soc. 51 (1955).
33. A. Lerf, H. He, M. Forster, J. Klinowski, Structure of graphite oxide revisited, J. Phys. Chem. B 102 (1998).
34. A.M. Rodríguez, P.S.V. Jiménez, Some new aspects of graphite oxidation at 0°c in a liquid medium. A mechanism proposal for oxidation to graphite oxide, Carbon 24 (1986).
35. B. Clarke, Normal bone anatomy and physiology., Clin. J. Am. Soc. Nephrol. CJASN 3 Suppl 3 (2008) S131-139.
36. L.T. Kuhn, M.D. Grynpas, C.C. Rey, Y. Wu, J.L. Ackerman, M.J. Glimcher, A comparison of the physical and chemical differences between cancellous and cortical bovine bone mineral at two ages, Calcif. Tissue Int. 83 (2008). https://doi.org/10.1007/s00223-008-9164-z.
37. J.E. Davies, Bone bonding at natural and biomaterial surfaces, Biomaterials 28 (2007).
38. J. Currey, The structure and mechanical properties of bone. In: Kokubo, T. (ed.) Bioceramics and their clinical applications, 2008.
39. M.I. Kay, R.A. Young, A.S. Posner, Crystal structure of hydroxyapatite, Nature 204 (1964).
40. J.Y. Kim, R.R. Fenton, B.A. Hunter, B.J. Kennedy, Powder diffraction studies of synthetic calcium and lead apatites, Aust. J. Chem. 53 (2000).
41. N. Rangavittal, A.R. Landa-Cánovas, J.M. González-Calbet, M. Vallet-Regí, Structural study and stability of hydroxyapatite and â-tricalcium phosphate: Two important bioceramics, J. Biomed. Mater. Res. 51 (2000).
42. S. Cazalbou, C. Combes, D. Eichert, C. Rey, Adaptative physico-chemistry of bio-related calcium phosphates, J. Mater. Chem. 14 (2004).
43. N. Abdullah, K. Hatano, D. Ando, K. Hirata, M. Kubo, A. Koshio, F. Kokai, Covalent Functionalization of Graphene Flakes with Well-Defined Azido-Terminated Poly(–-caprolactone) and Poly(2-oxazoline), Adv. Mater. Res. 1112 (2015).
44. N. Alzate-Carvajal, E.V. Basiuk, V. Meza-Laguna, I. Puente-Lee, M.H. Farías, N. Bogdanchikova, V.A. Basiuk, Solvent-free one-step covalent functionalization of graphene oxide and nanodiamond with amines, RSC Adv. 6 (2016) 113596–113610.
45. W.R. Collins, E. Schmois, T.M. Swager, Graphene oxide as an electrophile for carbon nucleophiles, Chem. Commun. 47 (2011).
46. S. Hou, S. Su, M.L. Kasner, P. Shah, K. Patel, C.J. Madarang, Formation of highly stable dispersions of silane-functionalized reduced graphene oxide, Chem. Phys. Lett. 501 (2010).
47. M.C. Hsiao, S.H. Liao, M.Y. Yen, P.I. Liu, N.W. Pu, C.A. Wang, C.C.M. Ma, Preparation of covalently functionalized graphene using residual oxygen-containing functional groups, ACS Appl. Mater. Interfaces 2 (2010). https://doi.org/10.1021/am100597d.
48. J. Jang, V.H. Pham, S.H. Hur, J.S. Chung, Dispersibility of reduced alkylamine-functionalized graphene oxides in organic solvents, J. Colloid Interface Sci. 424 (2014).
49. G.L. Li, G. Liu, M. Li, D. Wan, K.G. Neoh, E.T. Kang, Organo- and water-dispersible graphene oxide-polymer nanosheets for organic electronic memory and gold nanocomposites, J. Phys. Chem. C 114 (2010).
50. F. Pennetreau, O. Riant, S. Hermans, One-step double covalent functionalization of reduced graphene oxide with xanthates and peroxides, Chem. - Eur. J. 20 (2014).
51. S. Stankovich, R.D. Piner, S.B.T. Nguyen, R.S. Ruoff, Synthesis and exfoliation of isocyanate-treated graphene oxide nanoplatelets, Carbon 44 (2006).
52. K.S. Subrahmanyam, A. Ghosh, A. Gomathi, A. Govindaraj, C.N.R. Rao, Covalent and Noncovalent Functionalization and Solubilization of Graphene, Nanosci. Nanotechnol. Lett. 1 (2011).
53. Z. Xu, S. Wang, Y. Li, M. Wang, P. Shi, X. Huang, Covalent functionalization of graphene oxide with biocompatible poly(ethylene glycol) for delivery of paclitaxel, ACS Appl. Mater. Interfaces 6 (2014).
54. J. Yan, G. Chen, J. Cao, W. Yang, B. Xie, M. Yang, Functionalized graphene oxide with ethylenediamine and 1,6-hexanediamine, Carbon 52 (2013).
55. H. Yang, F. Li, C. Shan, D. Han, Q. Zhang, L. Niu, A. Ivaska, Covalent functionalization of chemically converted graphene sheets via silane and its reinforcement, J. Mater. Chem. 19 (2009).
56. M. Ayán-Varela, J.I. Paredes, L. Guardia, S. Villar-Rodil, J.M. Munuera, M. Díaz-González, C. Fernández-Sánchez, A. Martínez-Alonso, J.M.D. Tascón, Achieving extremely concentrated aqueous dispersions of graphene flakes and catalytically efficient graphene-metal nanoparticle hybrids with flavin mononucleotide as a high-performance stabilizer, ACS Appl. Mater. Interfaces 7 (2015).
57. S. Bose, T. Kuila, A.K. Mishra, N.H. Kim, J.H. Lee, Preparation of non-covalently functionalized graphene using 9-anthracene carboxylic acid, Nanotechnology 22 (2011).
58. P. Dubey, A. Kumar, R. Prakash, Non-covalent functionalization of graphene oxide by polyindole and subsequent incorporation of Ag nanoparticles for electrochemical applications, Appl. Surf. Sci. 355 (2015).
59. A.G. Hsieh, S. Korkut, C. Punckt, I.A. Aksay, Dispersion stability of functionalized graphene in aqueous sodium dodecyl sulfate solutions, Langmuir 29 (2013).
60. K. Jo, T. Lee, H.J. Choi, J.H. Park, D.J. Lee, D.W. Lee, B.S. Kim, Stable aqueous dispersion of reduced graphene nanosheets via non-covalent functionalization with conducting polymers and application in transparent electrodes, Langmuir 27 (2011).
61. D.W. Lee, T. Kim, M. Lee, An amphiphilic pyrene sheet for selective functionalization of graphene, Chem. Commun. 47 (2011).
62. N. Maity, A. Mandal, A.K. Nandi, Synergistic interfacial effect of polymer stabilized graphene via non-covalent functionalization in poly(vinylidene fluoride) matrix yielding superior mechanical and electronic properties, Polymer 88 (2016) 79–93.
63. G. Wang, X. Shen, B. Wang, J. Yao, J. Park, Synthesis and characterisation of hydrophilic and organophilic graphene nanosheets, Carbon 47 (2009).
64. Y. Yan, L. Piao, S.H. Kim, W. Li, H. Zhou, Effect of Pluronic block copolymers on aqueous dispersions of graphene oxide, RSC Adv. 5 (2015).
65. S.Z. Zu, D. Zhou, B.H. Han, Supramolecular surface modification and dispersion of graphene in water and organic solvents, in: 2013.
66. H.W. Kim, J.C. Knowles, H.E. Kim, Hydroxyapatite and gelatin composite foams processed via novel freeze-drying and crosslinking for use as temporary hard tissue scaffolds, J. Biomed. Mater. Res. - Part A 72 (2005).
67. M. Park, D. Lee, S. Shin, J. Hyun, Effect of negatively charged cellulose nanofibers on the dispersion of hydroxyapatite nanoparticles for scaffolds in bone tissue engineering, Colloids Surf. B Biointerfaces

130 (2015).
68. C.W. Chen, C.S. Oakes, K. Byrappa, R.E. Riman, K. Brown, K.S. TenHuisen, V.F. Janas, Synthesis, characterization, and dispersion properties of hydroxyapatite prepared by mechanochemical-hydrothermal methods, J. Mater. Chem. 14 (2004).
69. D.H. Kim, S.Y. Yoon, H.C. Park, Dispersion stability of hydroxyapatite-calcium phosphate glass ceramic-tertiary butyl alcohol system, in: 2014.
70. W. Noohom, K.S. Jack, D. Martin, M. Trau, Understanding the roles of nanoparticle dispersion and polymer crystallinity in controlling the mechanical properties of HA/PHBV nanocomposites, Biomed. Mater. 4 (2009).
71. X. Qiu, L. Chen, J. Hu, J. Sun, Z. Hong, A. Liu, X. Chen, X. Jing, Surface-modified hydroxyapatite linked by L-lactic acid oligomer in the absence of catalyst, J. Polym. Sci. Part Polym. Chem. 43 (2005) 5177–5185.
72. S. Baradaran, E. Moghaddam, B. Nasiri-Tabrizi, W.J. Basirun, M. Mehrali, M. Sookhakian, M. Hamdi, Y. Alias, Characterization of nickel-doped biphasic calcium phosphate/graphene nanoplatelet composites for biomedical application, Mater. Sci. Eng. C 49 (2015) 656–668.
73. D. Li, M.B. Müller, S. Gilje, R.B. Kaner, G.G. Wallace, Processable aqueous dispersions of graphene nanosheets, Nat. Nanotechnol. 3 (2008) 101–105.
74. S. Yang, X. Feng, S. Ivanovici, K. Müllen, Fabrication of graphene-encapsulated oxide nanoparticles: Towards high-performance anode materials for lithium storage, Angew. Chem. - Int. Ed. 49 (2010).
75. K.K. Kandori, A. Fudo, T. Ishikawa, Study on the particle texture dependence of protein adsorption by using synthetic micrometer-sized calcium hydroxyapatite particles, Colloids Surf. B Biointerfaces 24 (2002).
76. T. Kawasaki, Hydroxyapatite as a liquid chromatographic packing, J. Chromatogr. A 544 (1991).
77. M. Li, Q. Liu, Z. Jia, X. Xu, Y. Cheng, Y. Zheng, T. Xi, S. Wei, Graphene oxide/hydroxyapatite composite coatings fabricated by electrophoretic nanotechnology for biological applications, Carbon 67 (2014).
78. Y.Y. Shi, M. Li, Q. Liu, Z.J. Jia, X.C. Xu, Y. Cheng, Y.F. Zheng, Electrophoretic deposition of graphene oxide reinforced chitosan–hydroxyapatite nanocomposite coatings on Ti substrate, J. Mater. Sci. Mater. Med. 27 (2016).
79. S. Klébert, C. Balázsi, K. Balázsi, E. Bódis, P. Fazekas, A.M. Keszler, J. Szépvölgyi, Z. Károly, Spark plasma sintering of graphene reinforced hydroxyapatite composites, Ceram. Int. 41 (2015) 3647–3652.
80. P. Yu, R.Y. Bao, X.J. Shi, W. Yang, M.B. Yang, Self-assembled high-strength hydroxyapatite/graphene oxide/chitosan composite hydrogel for bone tissue engineering, Carbohydr. Polym. 155 (2017).
81. Y. Liu, Z. Dang, Y. Wang, J. Huang, H. Li, Hydroxyapatite/graphene-nanosheet composite coatings deposited by vacuum cold spraying for biomedical applications: Inherited nanostructures and enhanced properties, Carbon 67 (2014).
82. Y. Zeng, X. Pei, S. Yang, H. Qin, H. Cai, S. Hu, L. Sui, Q. Wan, J. Wang, Graphene oxide/hydroxyapatite composite coatings fabricated by electrochemical deposition, Surf. Coat. Technol. 286 (2016) 72–79.
83. Y. Li, C. Liu, H. Zhai, G. Zhu, H. Pan, X. Xu, R. Tang, Biomimetic graphene oxide-hydroxyapatite composites via in situ mineralization and hierarchical assembly, RSC Adv. 4 (2014).
84. F. Song, W. Jie, T. Zhang, W. Li, Y. Jiang, L. Wan, W. Liu, X. Li, B. Liu, Room-temperature fabrication of a three-dimensional reduced-graphene oxide/polypyrrole/hydroxyapatite composite scaffold for bone tissue engineering, RSC Adv. 6 (2016).
85. K. Benzerara, Biomineralization, in: M. Gargaud, W.M. Irvine, R. Amils, P. Claeys, H.J. Cleaves, M. Gerin, D. Rouan, T. Spohn, S. Tirard, M. Viso (Eds.), Encycl. Astrobiol., Springer Berlin Heidelberg, Berlin, Heidelberg, 2020: pp. 1–3.
86. A. Dey, G. de With, N.A.J.M. Sommerdijk, In situ techniques in biomimetic mineralization studies of calcium carbonate, Chem. Soc. Rev. 39 (2010) 397–409.
87. L.A. Estroff, Introduction: Biomineralization, Chem. Rev. 108 (2008) 4329–4331.
88. V.K. LaMer, R.H. Dinegar, Theory, Production and Mechanism of Formation of Monodispersed Hydrosols, J. Am. Chem. Soc. 72 (1950) 4847–4854.
89. E.D. EANES, I.H. GILLESSEN, A.S. POSNER, Intermediate States in the Precipitation of Hydroxyapatite, Nature 208 (1965) 365–367.
90. E. Hädicke, J. Rieger, I. Ursula Rau, D. Boeckh, Molecular dynamics simulations of the incrustation inhibition by polymeric additives, Phys. Chem. Chem. Phys. 1 (1999) 3891–3898.
91. O. Söhnel, J.W. Mullin, Precipitation of calcium carbonate, J. Cryst. Growth 60 (1982) 239–250.
92. W. Ostwald, Studien über die Bildung und Umwandlung fester Körper, 1 Abh. Übersättigung Überkaltung 22U (1897) 289–330.
93. J. Schroeder, C. Weingart, B. Coras, Clinical Journal of the American Society of Nephrology: CJASN, Clin J Am Soc … 7 (2012).
94. S. Mann, D.D. Archibald, J.M. Didymus, T. Douglas, B.R. Heywood, F.C. Meldrum, N.J. Reeves, Crystallization at Inorganic-organic Interfaces: Biominerals and Biomimetic Synthesis, Science 261 (1993) 1286–1292.
95. S. Weiner, W. Traub, A. Miller, D.C. Phillips, R.J.P. Williams, Macromolecules in mollusc shells and their functions in biomineralization, Philos. Trans. R. Soc. Lond. B Biol. Sci. 304 (1997) 425–434.
96. H. Liu, P. Xi, G. Xie, Y. Shi, F. Hou, L. Huang, F. Chen, Z. Zeng, C. Shao, J. Wang, Simultaneous reduction and surface functionalization of graphene oxide for hydroxyapatite mineralization, J. Phys. Chem. C 116 (2012).
97. J.D. Núñez, A.M. Benito, R. González, J. Aragón, R. Arenal, W.K. Maser, Integration and bioactivity of hydroxyapatite grown on carbon nanotubes and graphene oxide, Carbon 79 (2014) 590–604.
98. J. Zhao, Z. Zhang, Z. Yu, S. Yang, H. Jiang, Synthesis of hydroxyapatite on thioglycolic acid-capped reduced graphene oxide/silver nanoparticles: Effect of reaction condition in normal or pathological simulated body fluid, Mater. Lett. 116 (2014) 359–362.
99. T. Wen, X. Wu, M. Liu, Z. Xing, X. Wang, A.-W. Xu, Efficient capture of strontium from aqueous solutions using graphene oxide–hydroxyapatite nanocomposites, Dalton Trans. 43 (2014) 7464–7472.
100. H. Liu, J. Cheng, F. Chen, D. Bai, C. Shao, J. Wang, P. Xi, Z. Zeng, Gelatin functionalized graphene oxide for mineralization of hydroxyapatite: Biomimetic and in vitro evaluation, Nanoscale 6 (2014) 5315–5322.
101. H. Liu, J. Cheng, F. Chen, F. Hou, D. Bai, P. Xi, Z. Zeng, Biomimetic and cell-mediated mineralization of hydroxyapatite by carrageenan functionalized graphene oxide, ACS Appl. Mater. Interfaces 6 (2014) 3132–3140.
102. D. Depan, T.C. Pesacreta, R.D.K. Misra, The synergistic effect of a hybrid graphene oxide-chitosan system and biomimetic mineralization on osteoblast functions, Biomater. Sci. 2 (2014) 264–274.
103. F. Mohandes, M. Salavati-Niasari, Freeze-drying synthesis, characterization and in vitro bioactivity of chitosan/graphene oxide/hydroxyapatite nanocomposite, RSC Adv. 4 (2014).
104. M. Tavafoghi, N. Brodusch, R. Gauvin, M. Cerruti, Hydroxyapatite formation on graphene oxide modified with amino acids: arginine versus glutamic acid, J. R. Soc. Interface 13 (2016) 20150986.
105. Z. Fan, J. Wang, Z. Wang, Z. Li, Y. Qiu, H. Wang, Y. Xu, L. Niu, P. Gong, S. Yang, Casein phosphopeptide-biofunctionalized graphene biocomposite for hydroxyapatite biomimetic mineralization, J. Phys. Chem. C 117 (2013) 10375–10382.
106. J. Wang, Z. Ouyang, Z. Ren, J. Li, P. Zhang, G. Wei, Z. Su, Self-assembled peptide nanofibers on graphene oxide as a novel nanohybrid for biomimetic mineralization of hydroxyapatite, Carbon 89 (2015) 20–30.
107. J. Wang, H. Wang, Y. Wang, J. Li, Z. Su, G. Wei, Alternate layer-by-layer assembly of graphene oxide nanosheets and fibrinogen nanofibers on a silicon substrate for a biomimetic three-dimensional hydroxyapatite scaffold, J. Mater. Chem. B 2 (2014) 7360–7368.
108. F. Gao, C. Xu, H. Hu, Q. Wang, Y. Gao, H. Chen, Q. Guo, D. Chen, D. Eder, Biomimetic synthesis and characterization of hydroxyapatite/graphene oxide hybrid coating on Mg alloy with enhanced corrosion resistance, Mater. Lett. 138 (2015) 25–28.
109. E. Eisenbarth, P. Linez, V. Biehl, D. Velten, J. Breme, H.F. Hildebrand, Cell orientation and cytoskeleton organisation on ground titanium surfaces, Biomol. Eng. 19 (2002) 233–237.
110. P. Linez-Bataillon, F. Monchau, M. Bigerelle, H.F. Hildebrand, In vitro MC3T3 osteoblast adhesion with respect to surface roughness of Ti6Al4V substrates, Biomol. Eng. 19 (2002) 133–141.
111. T.J. Webster, T.A. Smith, Increased osteoblast function on PLGA composites containing nanophase titania, J. Biomed. Mater. Res. A 74A (2005) 677–686.
112. G.-Y. Chen, D.W.-P. Pang, S.-M. Hwang, H.-Y. Tuan, Y.-C. Hu, A graphene-based platform for induced pluripotent stem cells culture and differentiation, Biomaterials 33 (2012) 418–427.
113. W.C. Lee, C.H.Y.X. Lim, H. Shi, L.A.L. Tang, Y. Wang, C.T. Lim, K.P. Loh, Origin of enhanced stem cell growth and differentiation on graphene and graphene oxide., ACS Nano 5 (2011) 7334–7341.
114. O. Akhavan, E. Ghaderi, M. Shahsavar, Graphene nanogrids for selective and fast osteogenic differentiation of human mesenchymal stem cells, Carbon 59 (2013) 200–211.
115. S. Kang, J.B. Park, T.-J. Lee, S. Ryu, S.H. Bhang, W.-G. La, M.-K. Noh, B.H. Hong, B.-S. Kim, Covalent conjugation of mechanically stiff graphene

oxide flakes to three-dimensional collagen scaffolds for osteogenic differentiation of human mesenchymal stem cells, Carbon 83 (2015) 162–172.
116. T. Zhang, N. Li, K. Li, R. Gao, W. Gu, C. Wu, R. Su, L. Liu, Q. Zhang, J. Liu, Enhanced proliferation and osteogenic differentiation of human mesenchymal stem cells on biomineralized three-dimensional graphene foams, Carbon 105 (2016) 233–243.
117. N. Li, Q. Zhang, S. Gao, Q. Song, R. Huang, L. Wang, L. Liu, J. Dai, M. Tang, G. Cheng, Three-dimensional graphene foam as a biocompatible and conductive scaffold for neural stem cells, Sci. Rep. 3 (2013) 1604–1604.
118. S.Y. Park, J. Park, S.H. Sim, M.G. Sung, K.S. Kim, B.H. Hong, S. Hong, Enhanced Differentiation of Human Neural Stem Cells into Neurons on Graphene, Adv. Mater. 23 (2011) H263–H267.
119. S. Shah, P.T. Yin, T.M. Uehara, S.-T.D. Chueng, L. Yang, K.-B. Lee, Guiding stem cell differentiation into oligodendrocytes using graphene-nanofiber hybrid scaffolds., Adv. Mater. Deerfield Beach Fla 26 (2014) 3673–3680.
120. C.L. Weaver, X.T. Cui, Directed Neural Stem Cell Differentiation with a Functionalized Graphene Oxide Nanocomposite., Adv. Healthc. Mater. 4 (2015) 1408–1416.
121. L. Ahlinder, J. Henych, S.W. Lindström, B. Ekstrand-Hammarström, V. Stengl, L. Österlund, Graphene oxide nanoparticle attachment and its toxicity on living lung epithelial cells, RSC Adv. 5 (2015) 59447–59457.
122. Chang, S.-T. Yang, J.-H. Liu, E. Dong, Y. Wang, A. Cao, Y. Liu, H. Wang, In vitro toxicity evaluation of graphene oxide on A549 cells, Toxicol. Lett. 200 (2011) 201–210.
123. G. Lalwani, M. D'Agati, A.M. Khan, B. Sitharaman, Toxicology of graphene-based nanomaterials, Adv. Drug Deliv. Rev. 105 (2016) 109–144.
124. S.A. Redey, M. Nardin, D. Bernache-Assolant, C. Rey, P. Delannoy, L. Sedel, P.J. Marie, Behavior of human osteoblastic cells on stoichiometric hydroxyapatite and type A carbonate apatite: role of surface energy., J. Biomed. Mater. Res. 50 (2000) 353–364.
125. D. Turhani, M. Weissenböck, E. Watzinger, K. Yerit, B. Cvikl, R. Ewers, D. Thurnher, Invitro study of adherent mandibular osteoblast-like cells on carrier materials., Int. J. Oral Maxillofac. Surg. 34 (2005) 543–550.
126. Y.C. Shin, J.H. Lee, O.S. Jin, S.H. Kang, S.W. Hong, B. Kim, J.-C. Park, D.-W. Han, Synergistic effects of reduced graphene oxide and hydroxyapatite on osteogenic differentiation of MC3T3-E1 preosteoblasts, Carbon 95 (2015) 1051–1060.
127. J.H. Lee, Y.C. Shin, S.-M. Lee, O.S. Jin, S.H. Kang, S.W. Hong, C.-M. Jeong, J.B. Huh, D.-W. Han, Enhanced Osteogenesis by Reduced Graphene Oxide/Hydroxyapatite Nanocomposites, Sci. Rep. 5 (2015) 18833–18833.
128. J.H. Lee, Y.C. Shin, O.S. Jin, S.H. Kang, Y.-S. Hwang, J.-C. Park, S.W. Hong, D.-W. Han, Reduced graphene oxide-coated hydroxyapatite composites stimulate spontaneous osteogenic differentiation of human mesenchymal stem cells, Nanoscale 7 (2015) 11642–11651.
129. V. Ettorre, P. De Marco, S. Zara, V. Perrotti, A. Scarano, A. Di Crescenzo, M. Petrini, C. Hadad, D. Bosco, B. Zavan, L. Valbonetti, G. Spoto, G. Iezzi, A. Piattelli, A. Cataldi, A. Fontana, In vitro and in vivo characterization of graphene oxide coated porcine bone granules, Carbon 103 (2016) 291–298.
130. P. Duan, J. Shen, G. Zou, X. Xia, B. Jin, Biomimetic mineralization and cytocompatibility of nanorod hydroxyapatite/graphene oxide composites, Front. Chem. Sci. Eng. 12 (2018) 798–805.
131. Y. Chen, J. Ren, Y. Sun, W. Liu, X. Lu, S. Guan, Efficacy of graphene nanosheets on the plasma sprayed hydroxyapatite coating: Improved strength, toughness and in-vitro bioperformance with osteoblast, Mater. Des. 203 (2021) 109585.
132. P. Chandra Sekhar Boyapati, K. Srinivas, S. Akhil, Green synthesized graphene-hydroxyapatite nanocomposites for bioimplant applications, Mater. Lett. 327 (2022) 133059.
133. P.C.S. Boyapati, K. Srinivas, B. Chandu, Green synthesis of graphene-hydroxyapatite nanocomposites with improved mechanical properties for bone implant materials, Mater. Chem. Phys. 296 (2023) 127331.
134. Z. Fan, J. Wang, Z. Wang, H. Ran, Y. Li, L. Niu, P. Gong, B. Liu, S. Yang, One-pot synthesis of graphene/hydroxyapatite nanorod composite for tissue engineering, Carbon 66 (2014) 407–416.
135. S. Baradaran, E. Moghaddam, W.J. Basirun, M. Mehrali, M. Sookhakian, M. Hamdi, M.R.N. Moghaddam, Y. Alias, Mechanical properties and biomedical applications of a nanotube hydroxyapatite-reduced graphene oxide composite, Carbon 69 (2014) 32–45.
136. X. Xie, K. Hu, D. Fang, L. Shang, S.D. Tran, M. Cerruti, Graphene and hydroxyapatite self-assemble into homogeneous, free standing nanocomposite hydrogels for bone tissue engineering, Nanoscale 7 (2015) 7992–8002.
137. L. Crisan, B. Crisan, O. Soritau, M. Baciut, A.R. Biris, G. Baciut, O. Lucaciu, In vitro study of biocompatibility of a graphene composite with gold nanoparticles and hydroxyapatite on human osteoblasts, J. Appl. Toxicol. 35 (2015) 1200–1210.
138. C.C. Lopes, W.A. Pinheiro, D. Navarro da Rocha, J.G. Neves, A.B. Correr, J.R.M. Ferreira, R.M. Barbosa, J.R.F. Soares, J.L. Santos, M.H. Prado da Silva, Nanocomposite powders of hydroxyapatite-graphene oxide for biological applications, Ceram. Int. 47 (2021) 7653–7665.
139. I. Catelas, N. Sese, B.M. Wu, J.C.Y. Dunn, S. Helgerson, B. Tawil, Human mesenchymal stem cell proliferation and osteogenic differentiation in fibrin gels in vitro., Tissue Eng. 12 (2006) 2385–2396.
140. V. Chaturvedi, D. Naskar, B.F. Kinnear, E. Grenik, D.E. Dye, M.D. Grounds, S.C. Kundu, D.R. Coombe, Silk fibroin scaffolds with muscle-like elasticity support in vitro differentiation of human skeletal muscle cells., J. Tissue Eng. Regen. Med. 11 (2017) 3178–3192.
141. S.-J. Ding, M.-Y. Shie, C.-K. Wei, In vitro physicochemical properties, osteogenic activity, and immunocompatibility of calcium silicate-gelatin bone grafts for load-bearing applications., ACS Appl. Mater. Interfaces 3 (2011) 4142–4153.
142. G.I. Howling, P.W. Dettmar, P.A. Goddard, F.C. Hampson, M. Dornish, E.J. Wood, The effect of chitin and chitosan on the proliferation of human skin fibroblasts and keratinocytes in vitro, Biomaterials 22 (2001) 2959–2966.
143. T. Mori, M. Okumura, M. Matsuura, K. Ueno, S. Tokura, Y. Okamoto, S. Minami, T. Fujinaga, Effects of chitin and its derivatives on the proliferation and cytokine production of fibroblasts in vitro, Biomaterials 18 (1997) 947–951.
144. M. Li, Y. Wang, Q. Liu, Q. Li, Y. Cheng, Y. Zheng, T. Xi, S. Wei, In situ synthesis and biocompatibility of nano hydroxyapatite on pristine and chitosan functionalized graphene oxide, J. Mater. Chem. B 1 (2013) 475–484.
145. Y. Yan, X. Zhang, H. Mao, Y. Huang, Q. Ding, X. Pang, Hydroxyapatite/gelatin functionalized graphene oxide composite coatings deposited on TiO2 nanotube by electrochemical deposition for biomedical applications, Appl. Surf. Sci. 329 (2015) 76–82.
146. R. Deepachitra, R. Nigam, S.D. Purohit, B.S. Kumar, T. Hemalatha, T.P. Sastry, In Vitro Study of Hydroxyapatite Coatings on Fibrin Functionalized/Pristine Graphene Oxide for Bone Grafting, Mater. Manuf. Process. 30 (2015) 804–811.
147. M. Li, P. Xiong, M. Mo, Y. Cheng, Y. Zheng, Electrophoretic-deposited novel ternary silk fibroin/graphene oxide/hydroxyapatite nanocomposite coatings on titanium substrate for orthopedic applications, Front. Mater. Sci. 10 (2016) 270–280.
148. J. Luo, X. Zhang, J. Ong'achwa Machuki, C. Dai, Y. Li, K. Guo, F. Gao, Three-Dimensionally N-Doped Graphene-Hydroxyapatite/Agarose as an Osteoinductive Scaffold for Enhancing Bone Regeneration., ACS Appl. Bio Mater. 2 (2019) 299–310.
149. A. Sanati, A. Kefayat, M. Rafienia, K. Raeissi, R. Siavash Moakhar, M.R. Salamat, S. Sheibani, J.F. Presley, H. Vali, A novel flexible, conductive, and three-dimensional reduced graphene oxide/polyurethane scaffold for cell attachment and bone regeneration, Mater. Des. 221 (2022) 110955.
150. Y. Liu, J. Huang, H. Li, Nanostructural Characteristics of Vacuum Cold-Sprayed Hydroxyapatite/Graphene-Nanosheet Coatings for Biomedical Applications, J. Therm. Spray Technol. 23 (2014) 1149–1156.
151. Liu, J. Huang, H. Li, Synthesis of hydroxyapatite-reduced graphite oxide nanocomposites for biomedical applications: oriented nucleation and epitaxial growth of hydroxyapatite., J. Mater. Chem. B 1 (2013) 1826–1834.
152. L. Zhang, W. Liu, C. Yue, T. Zhang, P. Li, Z. Xing, Y. Chen, A tough graphene nanosheet/hydroxyapatite composite with improved in vitro biocompatibility, Carbon 61 (2013) 105–115.
153. M. Gong, Q. Zhao, L. Dai, Y. Li, T. Jiang, Fabrication of polylactic acid/hydroxyapatite/graphene oxide composite and their thermal stability, hydrophobic and mechanical properties, J. Asian Ceram. Soc. 5 (2017) 160–168.
154. C. Shuai, B. Peng, P. Feng, L. Yu, R. Lai, A. Min, In situ synthesis of hydroxyapatite nanorods on graphene oxide nanosheets and their reinforcement in biopolymer scaffold, J. Adv. Res. 35 (2022) 13–24.
155. F. Shadianlou, A. Foorginejad, Y. Yaghoubinezhad, Fabrication of zirconia/reduced graphene oxide/hydroxyapatite scaffold by rapid prototyping method and its mechanical and biocompatibility properties, Ceram. Int. 48 (2022) 7031–7044.
156. M.T. Elabbasy, F.D. Algahtani, H.F. Alshammari, L. Kolsi, M.A. Dkhil,

G.I. Abd El-Rahman, M.A. El-Morsy, A.A. Menazea, Improvement of mechanical and antibacterial features of hydroxyapatite/chromium oxide/graphene oxide nanocomposite for biomedical utilizations, Surf. Coat. Technol. 440 (2022) 128476.
157. H. Lee, J.M. Yoo, N.K. Ponnusamy, S.Y. Nam, 3D-printed hydroxyapatite/gelatin bone scaffolds reinforced with graphene oxide: Optimized fabrication and mechanical characterization, Ceram. Int. 48 (2022) 10155–10163.
158. B. Flora, R. Kumar, P. Tiwari, A. Kumar, J. Ruokolainen, A.K. Narasimhan, K.K. Kesari, P.K. Gupta, A. Singh, Development of chemically synthesized hydroxyapatite composite with reduced graphene oxide for enhanced mechanical properties, J. Mech. Behav. Biomed. Mater. 142 (2023) 105845.
159. A. Babakhani, S.J. Peighambardoust, A. Olad, Fabrication of magnetic nanocomposite scaffolds based on polyvinyl alcohol-chitosan containing hydroxyapatite and clay modified with graphene oxide: Evaluation of their properties for bone tissue engineering applications, J. Mech. Behav. Biomed. Mater. 150 (2024) 106263.
160. J. Dusza, J. Morgiel, A. Duszová, L. Kvetková, M. Nosko, P. Kun, C. Balázsi, Microstructure and fracture toughness of Si3N4+graphene platelet composites, J. Eur. Ceram. Soc. 32 (2012) 3389–3397.
161. L. Kvetková, A. Duszová, P. Hvizdoš, J. Dusza, P. Kun, C. Balázsi, Fracture toughness and toughening mechanisms in graphene platelet reinforced Si3N4 composites, Scr. Mater. 66 (2012) 793–796.
162. J. Liu, H. Yan, M.J. Reece, K. Jiang, Toughening of zirconia/alumina composites by the addition of graphene platelets, J. Eur. Ceram. Soc. 32 (2012) 4185–4193.
163. L.S. Walker, V.R. Marotto, M.A. Rafiee, N. Koratkar, E.L. Corral, Toughening in Graphene Ceramic Composites, ACS Nano 5 (2011) 3182–3190. https://doi.org/10.1021/nn200319d.
164. G.B. Yadhukulakrishnan, S. Karumuri, A. Rahman, R.P. Singh, A. Kaan Kalkan, S.P. Harimkar, Spark plasma sintering of graphene reinforced zirconium diboride ultra-high temperature ceramic composites, Ceram. Int. 39 (2013) 6637–6646. https://doi.org/10.1016/j.ceramint.2013.01.101.
165. Y. Zhao, K.N. Sun, W.L. Wang, Y.X. Wang, X.L. Sun, Y.J. Liang, X.N. Sun, P.F. Chui, Microstructure and anisotropic mechanical properties of graphene nanoplatelet toughened biphasic calcium phosphate composite, Ceram. Int. 39 (2013) 7627–7634.
166. I. Bajpai, D.Y. Kim, Y.H. Han, B.K. Jang, S. Kim, Directional property evaluation of spark plasma sintered GNPs-reinforced hydroxyapatite composites, Mater. Lett. 158 (2015) 62–65.
167. N. Nomura, K. Sakamoto, K. Takahashi, S. Kato, Y. Abe, H. Doi, Y. Tsutsumi, M. Kobayashi, E. Kobayashi, W.-J. Kim, K.-H. Kim, T. Hanawa, Fabrication and Mechanical Properties of Porous Ti/HA Composites for Bone Fixation Devices, Mater. Trans. 51 (2010) 1449–1454.
168. A. Jankoviæ, S. Erakoviæ, M. Mitriæ, I.Z. Matiæ, Z.D. Juraniæ, G.C.P. Tsui, C. Tang, V. Miškoviæ-Stankoviæ, K.Y. Rhee, S.J. Park, Bioactive hydroxyapatite/graphene composite coating and its corrosion stability in simulated body fluid, J. Alloys Compd. 624 (2015) 148–157.
169. L. Zhang, X.G. Zhang, Y. Chen, J.N. Su, W.W. Liu, T.H. Zhang, F. Qi, Y.G. Wang, Interfacial stress transfer in a graphene nanosheet toughened hydroxyapatite composite, Appl. Phys. Lett. 105 (2014) 161908–161908.
170. H. Zanin, E. Saito, F.R. Marciano, H.J. Ceragioli, A.E. Campos Granato, M. Porcionatto, A.O. Lobo, Fast preparation of nano-hydroxyapatite/superhydrophilic reduced graphene oxide composites for bioactive applications, J. Mater. Chem. B 1 (2013) 4947–4955.
171. S.H. Song, K.H. Park, B.H. Kim, Y.W. Choi, G.H. Jun, D.J. Lee, B.S. Kong, K.W. Paik, S. Jeon, Enhanced thermal conductivity of epoxy-graphene composites by using non-oxidized graphene flakes with non-covalent functionalization, Adv. Mater. 25 (2013).
172. H. Gao, S. Zhang, F. Lu, H. Jia, L. Zheng, Aqueous dispersion of graphene sheets stabilized by ionic liquid-based polyether, Colloid Polym. Sci. 290 (2012).
173. G. Xiong, H. Luo, G. Zuo, K. Ren, Y. Wan, Novel porous graphene oxide and hydroxyapatite nanosheets-reinforced sodium alginate hybrid nanocomposites for medical applications, Mater. Charact. 107 (2015) 419–425.